Zircon Lu-Hf constraints on recently proposed models for the tectonic assembly of Proterozoic central Australia

Thesis submitted in accordance with the requirements of the
University of Adelaide for an Honours Degree in Geology

Claire Michelle Thomas

November 2012

THE UNIVERSITY of ADELAIDE

ZIRCON LU-HF CONSTRAINTS ON RECENTLY PROPOSED MODELS FOR THE TECTONIC ASSEMBLY OF PROTEROZOIC CENTRAL AUSTRALIA

U-PB AND ZIRCON LU-HF FROM CASEY INLIER

ABSTRACT

The Arunta region, central Australia, is interpreted to record evidence for the complex evolution and growth of the Australian continent during the Paleoproterozoic and Mesoproterozoic. The Warumpi Province, in the southern Arunta region, has been proposed to be an exotic terrain that has accreted to the more northerly Aileron Province in the North Australian Craton during the ca1640 Ma Liebig Orogeny.

The Casey Inlier has been identified to contain the boundary between the Aileron and Warumpi Provinces. U-Pb dating indicates ages of ca1652-1670 Ma granites to be the Warumpi Province and the ca1756-1774 Ma granitic to be the Aileron Province. New Lu-Hf zircon analysis undertaken in this study revealed that the source regions of both provinces are isotopically indistinguishable. U-Pb and Lu-Hf analysis of detrital zircon in a quartzite cover sequence provides a maximum depositional age of ca1311 Ma and an isotopic signature that is characteristic of the Musgrave Province. This suggests that the Arunta region was proximal at this time. Field observation indicate a pervasive NNW-SSE strike fabric with east side up shear dated at ca 1730 Ma age, with a later west side up shear fabric attributed to be ca 1140 Ma shear fabric. The data obtained in this study combined within previous evidence for shared histories indicate the Warumpi Province was not exotic to the Aileron Province and it is most unlikely that a suturing event occurred at ca 1640 Ma.

KEYWORDS

Aileron, Warumpi, Casey Inlier, Lu-Hf, U-Pb, Zircon

TABLE OF CONTENTS

LIST OF FIGURES AND TABLES

INTRODUCTION

The Casey Inlier in central Australia is thought to preserve a ca 1640 Ma suture (Close *et al.* 2004) between the ca 1830-1780 Ma Aileron Province, southern Northern Australian Craton (NAC), and the 1690-1600 Ma Warumpi Province, which is potentially an exotic terrane (Close *et al.* 2004, Scrimgeour *et al.* 2005). The suture has been proposed to have been a smaller continental fragment that would have accreted on to the NAC (Selway et al. 2006) (Figure 1). Little work has been done on the boundary between the two provinces despite its implied importance in the development of central Australia. This is largely due to overprinting events and restricted land access due to native title landholdings. The Casey lnlier is an ideal location to study the proposed suture as it is in an easily accessible study area located on pastoral lands and the western domain is determined to be the Warumpi Province and the Eastern and Central Domains to be the Aileron Province by Carson *et al.* (2009)

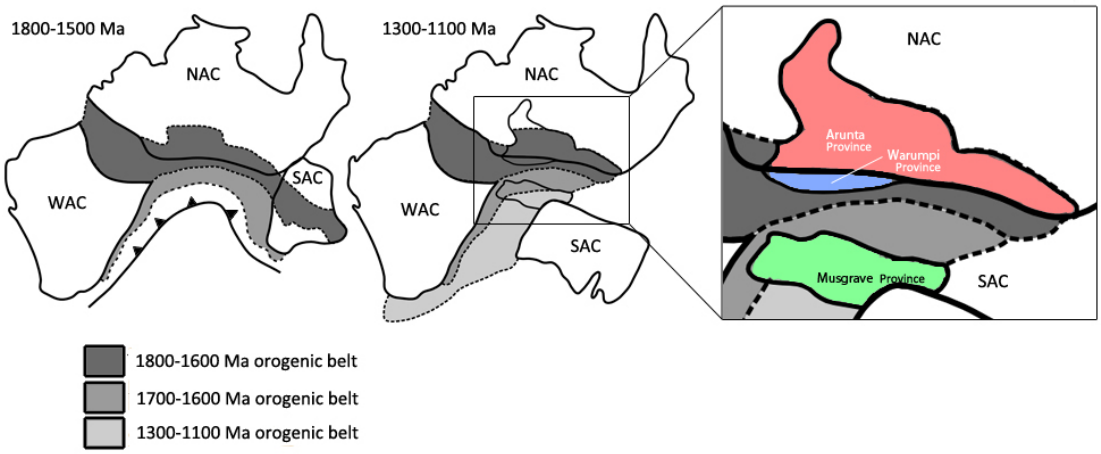

Figure 1: Proposed suturing during the1800-1500 Ma where there is a proposed north dipping subduction under the North Australian Craton (NAC) and the merger of the South Australian Craton (SAC) and the Western Australian Craton (WAC). Followed by the merger of the further addition of the SAC to create the Musgrave Province during 1300-1100 Ma. The corresponding orogensis during 1800-1600 Ma in the dark grey, 1700-1600 Ma in the grey and 1300-1100 Ma in the light grey. Adapted from Giles *et al.* (2004).

The suture of the Warumpi Provence and the Aileron Provence has been hypothesises to have occurred during the ca 1640 Ma Liebig Orogeny (Scrimgeour *et al.* 2005). The evidence for this proposed suture has been; 1. two distinctive protolith ages of different provinces, 2, distinctive Sm-Nd isotopic signature of the two different provinces (Close *et al.* 2004), 3. magnetotelluric data with interpreted fossil subduction-style system (Selway *et al.* 2009), 4. a hair pin bend in the apparent polar wander path (Idnurm 2000) and 5. moderate to high pressure metamorphism with associated voluminous magmatism at ca 1640-1635 Ma (Scrimgeour *et al.* 2005).

This study aims to identify if a suture event occurred during the Liebig Orogeny or at some stage during the Paleoproterozoic or Mesoproterozoic. This will be done by identifying the relationship between the rocks of the Western, Eastern and Central Domains of the Casey Inlier which are proposed to be the Warumpi Province juxtaposing the Aileron Province in the Casey Inlier. To do this, investigating the age and inherited zircon ages of rocks from the Warumpi Province in the Casey Inlier, coupled with Lu-Hf isotope analysis will characterise the protolith age of the rocks. If the Warumpi and Aileron Provinces have significantly differing Hf isotopic characteristics then it will support the notion that the Warumpi Province is an exotic terrain that has accreted on to the Aileron Province. If the isotopic compositions are similar it suggests that the granitic rocks simple indicate remelting of the Aileron Province. Field investigation, monazite geochronology and zircon geochronology will be used in determining the age of metamorphism in the region.

Overlying the Paleoproterozoic rocks of the central Casey Inlier is a muscovite-bearing quartzite deposited ≤1235±74 Ma , with a NNW-SSE fabric (Close *et al.* 2007). The detrital zircons within this sedimentary unit yield ages ranging from ca 1230-1850 Ma, with age peaks at ca1350 Ma, 1550 Ma, 1660 Ma, 1700 Ma and 1750 Ma. These zircon ages are restricted to within the NAC and also common in the Musgrave Province (Wade *et al.* 2006, Carson *et al.* 2009, Kirkland *et al.* 2012). U-Pb geochronology coupled with Lu-Hf isotope data, will potentially reveal the relationship between the Warumpi, Aileron and Musgrave Province, and provide insight in to the poorly understood development in central Australia during the Mesoproterozoic.

GEOLOGICAL SETTING

Formation of the Arunta region

The Arunta region has been divided into the Aileron and Warumpi Provinces which have complex tectonic historieS (Table 1). The Arunta region is a polymetamorphic region that is found in the south of the NAC (Collins & Shaw 1995, Scrimgeour 2003) (Figure 2), and is evidently in a pivotal position to investigate the growth of northern Australia. The Arunta region has been divided into the Aileron Province and the Warumpi Province.

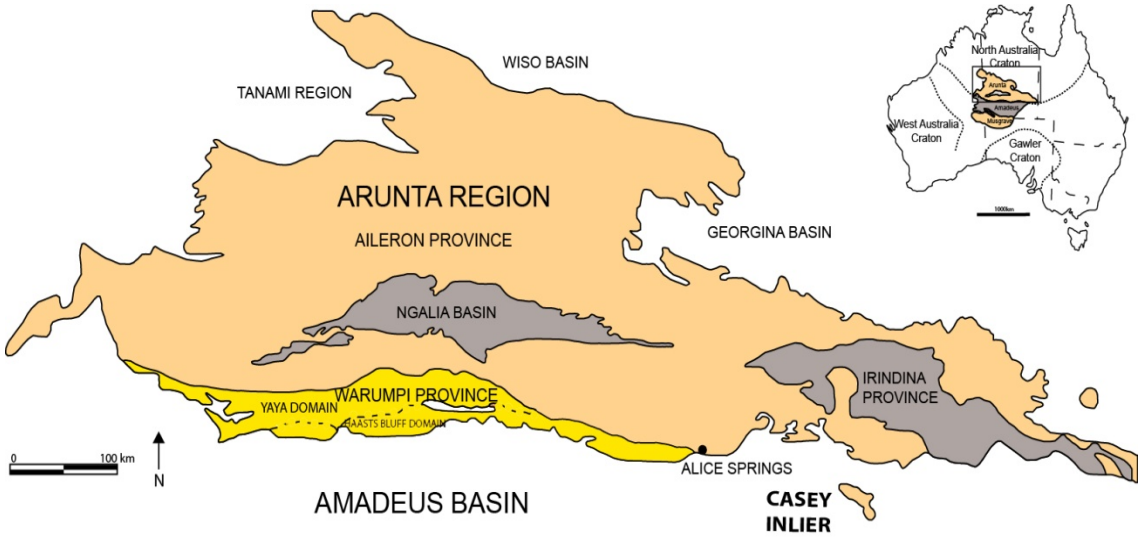

Figure 2: Location of the Arunta Region in Australia and the locations Aileron Province, Warumpi Province and Casey Inlier. This image is adapted from Scrimgeour 2005.

The Aileron Province has undergone multiple deformation events (Pietsch 2001, Claoué-Long 2003, Scrimgeour 2003). The Aileron Province outcrops consist of low upper greenschist facies rocks juxtaposed to high grade granulite facies rocks (Claoué-Long *et al.* 2008). During ca 1865-1820 Ma the Aileron Province has been interpreted to be a broad basin with no moving depocenters, that latter has been proposed to move gradually moved southwards into which sediment from the NAC was deposited (Scrimgeour *et al.* 2005), which is now identified predominantly as the Lander Package (Claoué-Long & Hoatson 2005). These basins have a proposed Archean basement (Scrimgeour *et al.* 2005). During ca 1840-1810 Ma the proposed basin had a deep marine setting that developed into a shallow marine system by ca 1810-1800 Ma. Between ca 1805-1800 Ma felsic and mafic intrusions were widespread throughout the area which developed into clastic and volcaniclastic sedimentation with marine transgression between ca 1790-1780 Ma. In the eastern and southern part of the Arunta between ca 1760-1740 Ma felsic and minor mafic magmatism occurred, which has been

proposed to have formed in the back-arc environment before the Strangways Event (Scrimgeour *et al.* 2005)

The Warumpi Province is situated on the southern margin of the NAC neighbouring the Aileron Province (Shaw *et al.* 1984), but it is separated by the Charles River Thrust, Redbank Thrust and Desert Bore Shear Zone which are consider to be part of the Central Australian Suture (Scrimgeour *et al.* 2005). It consists of two domains the Haast Bluff Domain deposited characterised by sequences felsic intrusive volcanics between ca 1690-1660 Ma and ca 1630-1610 Ma and the Yaya domain which contains sequences deposited between ca 1660-1640 Ma (Scrimgeour 2003, Scrimgeour *et al.* 2005) (Figure 2).

The Arunta region is a complex geological area with an igneous, metamorphic and tectonic history. This has been outlined in table 2.

Table 1: Summary of Palaeo-Mesoproterozoic tectonic events in central Australia

Name	Age	Regional Distribution	Magmatism	Metamorphic Character	Deformation
Stafford Event	1810-1800 Ma (Claoué-Long & Hoatson 2005)	Central and northern Aileron Province	Granitic and mafic	Granulite facies with low P highT with a max PT 850°C and 3 kbar	Low strain mainly thermal event
Yambah Event	1780-1760 Ma (Claoué-Long & Hoatson 2005)	Central and southern Aileron Province	Granitic and mafic	Granulite grade with low-medium P, high T and an unknown max PT	Compression
Inkamulla Igneous Event	1760-1740 Ma (Scrimgeour et al 2003)	South-eastern Aileron Province	Granitic and mafic includes apparent arc related with A-type magmatism	Metamorphic character not known	Not yet obtained
Early Strangways Orogeny	1730-1715 Ma (Claoué-Long *et al.* 2008))	South-eastern and southern Aileron Province	Minor felsic magmatism	Granulite grade with low-medium P, high T with a max PT poorly defined	Regional high-grade deformation event predominantly compression
Late Strangways Orogeny	1700-1670 Ma (Claoué-Long *et al.* 2008)	South-eastern and southern Aileron Province	Abundant mafic dykes	Granulite grade with a medium PT up to with a max PT 800°C and 7kbar	Mylonitic regions and large scale folds associated with east-west extension

Argilke Igneous Event	1690-1670 Ma (Scrimgour 2003)	Southern Warumpi Province (Scrimgeour et al 2005)	Volumetrically significant predominantly felsic magmatism	Upper amphibolite grade with a metamorphic character poorly defined, but up to	Not yet obtained
Leibig Orogeny	1640-1630 Ma (Scrimgour *et al.* 2005)	Central Warumpi Province and southern Aileron Province (Scrimgeour *et al.* 2005; Wong, 2011)	Volumetrically significant predominantly felsic magmatism and mafic to ultramafic magmatism	Granulite grade with a metamorphic grade poorly defined, but locally up to high PT granulite with a max PT 900°C and 9kbar	Not yet obtained
Ormiston event	1620-1600 Ma (Scrimgour 2003)	Southern Warumpi Province (Scrimgeour *et al.*2005)	Volumetrically significant predominantly felsic magmatism, with a relatively juvenile character	Metamorphic character unknown	Not yet obtained
Chewings Orogeny	1600-1550 Ma (Hand & Buick 2001, Claoué-Long *et al.* 2008)	Central Warumpi Province and southern and central Aileron Province (Hand & Buick 2001, Wong 2011)	Minor felsic magmatism in high-grade metamorphic grade in the Central Aileron Province and volumetrically significant felsic magmatism in the Central western Aileron Province	Granulite grade with a max PT 850°c and 6 kbar	Compression with regions associated with top to the south transport
Teapot Event	1160-1130 Ma (Morrissey *et al.*, 2011)	Warumpi Province and southern Aileron Province	Felsic to mafic and ultramafic	Amphibolite to granulite with a max PT 800°C and 6 kbar	Compression with E-W trending isoclinal folding

During the Liebig Orogeny ca 1640-1635 Ma the Warumpi Provence is proposed to have been an exotic terrain accreted on to the Aileron Provence (Scrimgeour *et al.* 2005). Interpretation has been based on evidence of high-temperature, moderate to high pressure metamorphism which is associated with voluminous magmatism and isothermal decompression (Scrimgeour *et al.* 2005). Arc like geochemical signatures of granites found in the Arunta region (Zhao & Bennett 1995, Zhao & McCulloch 1995) suggests that the NAC was the overriding plate in a north- dipping subduction system during the Paleoproterozoic (Karlstrom *et al.* 2001, Giles *et al.* 2002, Giles *et al.* 2004, Betts & Giles 2006). Further evidence Warumpi Province is exotic to the NAC is the apparent lack of Archean inheritance in granites and a less evolved isotopic signature (Close *et al.* 2004). This feature has been interpreted to represent a fossil subduction-style system that may have been involved in the suture between the Aileron and Warumpi Province (Selway *et al.* 2009). Magnetotelluric data provides evidence of a lithopspheric scale south dipping feature which has been interpreted to have been

initially a north dipping subduction feature, until ca 1700 Ma when it changed orientation to become a south dipping structure. The timing of the Leibig Orogeny also corresponds with a hair pin bend in the apparent polar wander path and this change in the polar wander path has been interpreted as a change in the direction of plate movement (Idnurm 2000), potentially related to a collisional orogenic event (Scrimgeour *et al.* 2005).

Evidence suggesting that the Warumpi Province is exotic to the NAC appears convincing. Evidence suggests it could alternatively be an extended region of the Aileron Province supported by, detrital zircon ages obtained from the Warumpi Province are similar to those found in the Aileron Province (Claoué-Long *et al.* 2008) and by granites of Leibig orogeny age intrude the Aileron Province (Wong 2011), suggesting that the Warumpi age magmatism is not constrained to the Warumpi Province (Claoué-Long & Hoatson 2005).

This project aims to examine the relationship between the Warumpi Province and the Aileron Province in the Casey Inlier, as well as its association with the cover sequence.

Geological setting and field observations of this study area

The Casey Inlier is an isolated part of the Arunta Region located to the south east of the Arunta Region on the N-E side of the Hale River in the Amadeus Basin (Close *et al.* 2006). The Casey Inlier consists of three domains which are categorised by Close *et al.* (2006) with regards to structural boundaries, metamorphic grade and protolith. There is also a muscovite-bearing quartzite cover sequence (Figure 3).

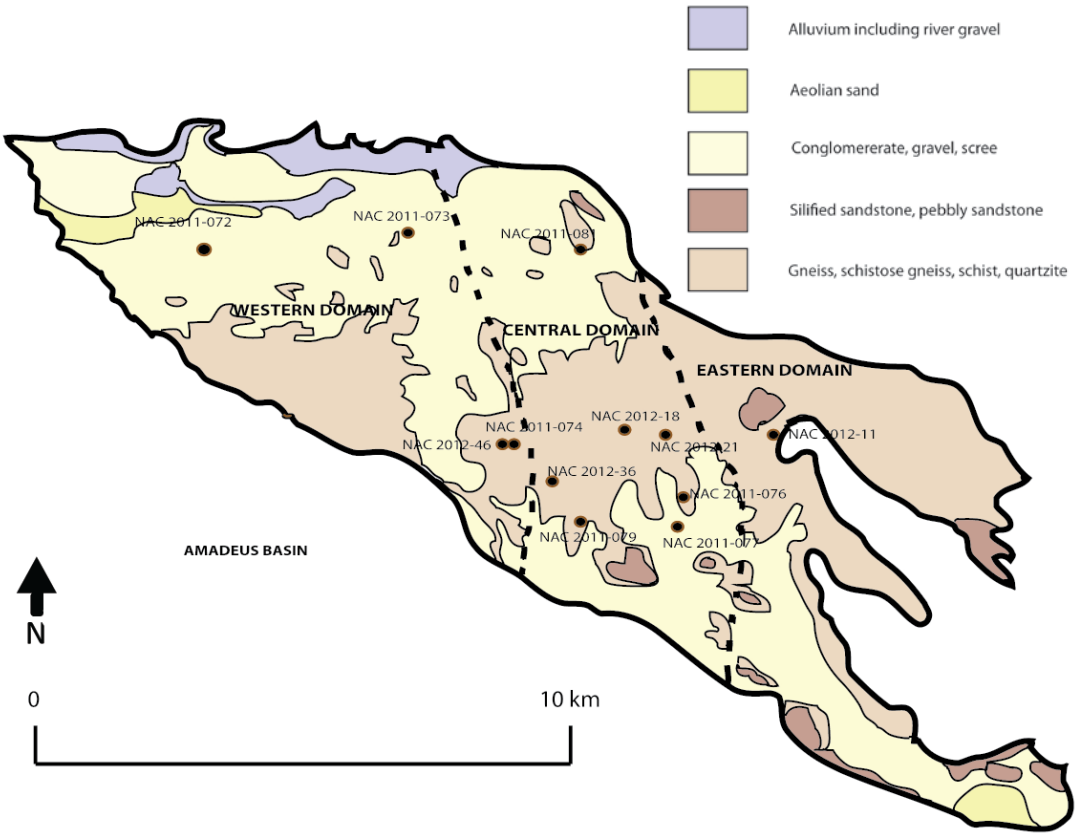

Figure 3: Simplified geology of the Casey Inlier indicating the Warumpi Provence in the west and the Aileron Province in the east. Locations of samples are marked.

Eastern Domain

This domain contains by upper amphibolite facies rocks that are characterised by quartz, plagioclase and biotite. Minor metasedimentary lithologies contain garnet, biotite and sillimanite. The felsic lithologies may be meta-igneous, and in places more than 100m wide metagabbros have intruded the felsic lithologies. These have been reworked to form gneiss with a variation in intensity and in some areas boudinaged melt veins (Figure 4a, 4b). In places it is evident that this foliation has overprinted an earlier high-grade metamorphic fabric. This is best seen by the partial preservation of garnet bearing leucosomes in biotite- sillimanite bearing metasediments (Figure 4c).

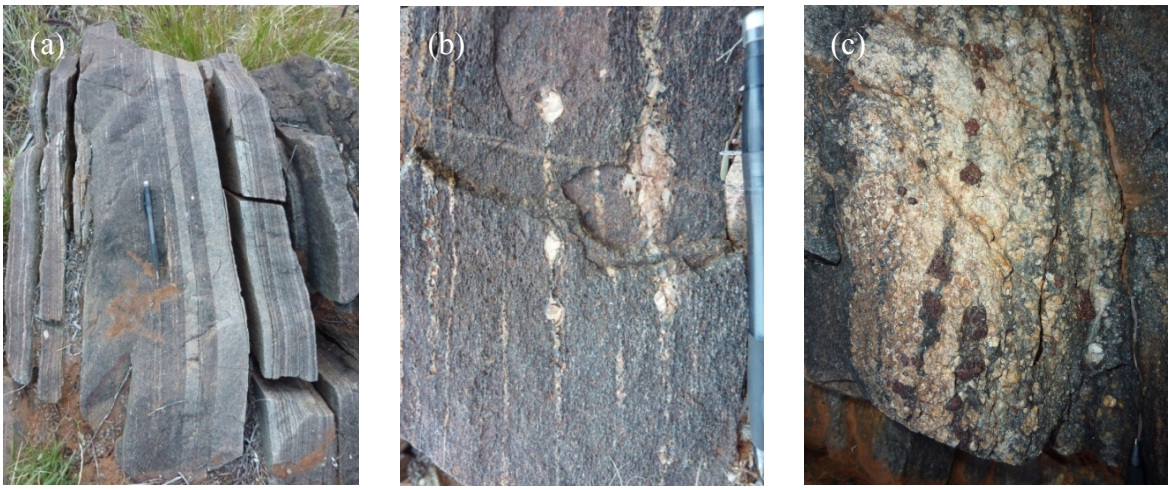

Figure 4: The gneissic fabric with increasing strain evident in a, and boudinaged melt veins created from the strain in a and increasing strain evident in b, and c) shows a leucosome with a biotite-sillimanite bearing metasediment which a NNW-SSE fabric overprint.

This domain contains a pervasive NNW-SSE trending foliation with high angle SW dip. The foliation has been locally reworked by layered parallel phyllonitic ≤5m wide shear zones that generally have a dip slip east-side up movement (Figure 5a).

The fabric contains 2 generations of pegmatite veins (Figure 5b). The first is a highly deformed layer parallel to the foliation and the second intrudes at a high angle into the fabric and is cross cut by the phyllonitic shear zones.

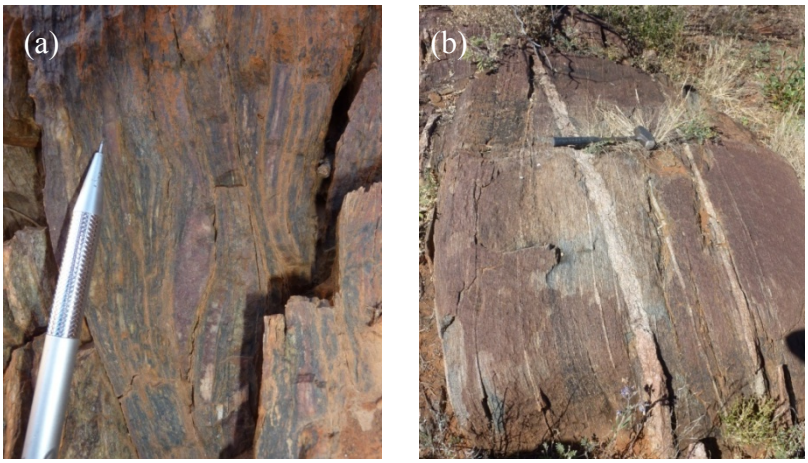

Figure 5: East-side up sigma clasts a, and 2 generations of pegmatite veins which cross cut each other.

There are also series of different veins that cross cut the fabric in this domain such as Carbonate veins which are up to 7m wide. Ultra-mafic intrusions of Gabbro are found in elongate boudinaged up to 10m wide, which could be the earliest veining in the area.

Detrital zircon ages in metasediments are similar to those recorded from the Lander Rock Formation (Carson *et al.* 2009), with a maximum deposition age of ca 1845 Ma. The felsic gneisses are interpreted to have igneous protoliths which give an age of 1817±4 Ma.

Central Domain

The central domain of the Casey Inlier is characterised by a highly migmatised granulite facies metasediments that have been intruded by mafic rocks which for bodies up to 1.5 km by 1 km. The migmatites are garnet-sillimanite-biotite bearing assemblages and are in places diatexitic. They contain a weakly defined approximately E-W to NNE-SSW, steeply S–dipping layering which is defined by felsic veins, with remnants of the primary lithological layering as rough elongations. Contact between the mafic rock and the migmatised metasediments is found, the mafic rock has mixed with the diatexite forming textures reminiscent of magma mingling.

The metasedimentary rocks have been intruded by megacrystic granites indicating that they postdate the partial melting of the metasediments. This indicates that there has not been mixing between the granites and metasediments (Figure 6a). The boundaries of the Central Domain have high grade metasediments and igneous protoliths which have been overprinted by a pervasive NNW-SSE trending foliation. The megacrystic granites as a result of this have formed domains of highly strained augen gneiss up to 700m

wide, which are defined by biotite, quartz ribbons and elongation of the K-feldspars (Figure 6b). This fabric is most evident along the eastern side of the Central Domain and has an east-side up movement indicator along a steeply plunging lineation. This is parallel to a well developed amphibolites-grade foliation which has been overprinted by an earlier high-grade mineral assemblage in the Eastern Domain.

Figure 6: Metasedimentary rock which has been intruded by megacrystic melt fragments, surrounded by melt halos, in image a and image b an e ast side up sigma clasts of K-feldspar, of highly strained augen gneiss defined by biotite and quartz ribbons.

The east side up foliations in places has been reworked by micaeous shear zones, which are defined by muscovite-biotite foliations, as well as been retrogressed in areas up to 20m wide possessing opposite shear sense along a steeply plunging lineation. The younger shear zones are associated with the retrograde assemblage from ~25% of the foliation system that overprints the earlier high-grade metamorphic rocks and granites.

The detrital zircon age spectra from the migmatised metasediments are similar to the sedimentary derived lithologies in the Aileron Province, gibing a maximum depositional

age of around 1865±5 Ma (Carson *et al.* 2009). The high-grade metamorphism in the Central Domain overlapped with the 1770.6± 4.4 Ma of the gabbro's, which display a syn-metamorphic relationship with the enclosing migmatites, speculated to be a result of the of their intrusions (Carson *et al.* 2009).

The boundary between the Central and Eastern Domains is a sequence of quartzite that forms a prominent set of steeply dipping NNW-SEE trending strike ridges. The quartzite package is ~150 m thick, containing individual quartzite units which are several meters thick and separated by impure quartzite. This sequence is associated with fine-grained muscovite, garnet and staurolite-bearing porphyroblastic metapelite. The intense recrystallisation has preserved sedimentary structures, but in some places there is still graded bedding indicating an upright stratigraphy.

The quartzite cover defines an upright macroscopic, gently north-plunging isoclinal syn-form with preserved limb lengths of around 8km. Within muscovite-bearing quartzite, the upright NNW-SS trending foliation is axial surface to the macroscopic fold, overprints an earlier cleavage indicating that the regional scale fold is an F2 structure (Figure 7a). This simple F2 folds geometry suggests that F1 structures were either small scale or that S1 was overall layer parallel (Figure 7b).

Figure 7: Isoclinal fold of an F2 structure in figure a, which have been overprinted by cleavages forming F1 in, in figure b shows small crenulations in the quartzite beds and smaller S1 shears.

Detrital zircon ages indicate that the quartzite has a maximum depositional age of ca 1270 Ma (Carson *et al.* 2009). The eastern limb of the fold is unconformably overlies the basement of the Amadeus Basin (ca 830 Ma), indicating that deformation occurred between the late Mesoproterozoic-early Neoproterozoic.

Western Domain

This domain is dominated by granite and granitic gneiss. Contact with the Central Domain is along a zone of variably foliated greenschist facies retrogression which is several hundred meters wide. It has overprinted an earlier shear fabric that is developed across the domain > 2km wide along the eastern margin of the western domain.

The shear fabric is sub-vertical and trends NNW-SSE. In areas of low deformation intensity, the granites are weakly foliated with large K-feldspar phenocrysts, or are even

grained. These granites are converted into augen gneiss or pervasively foliated granitic gneiss with increasing strain. At high strains the rocks have an intense foliation defined by biotite, ribbons of quartz and feldspar which envelop K-feldspar porphyroclasts. The fabric increases in intensity in non Augen gneiss areas which is characterised by the development of a coarse-grained (1-3 mm) muscovite-biotite bearing foliation. In muscovite rich shear zones, mylonitised quartz veins are common. Kinematic indicators (S-C fabrics, sigma and delta clasts) all present a west-side-up movement along a steeply plunging lineation (Figure 8).

Figure 8: Sigma clasts of K-feldspar porphroclasts with foliation defined by biotite, ribbons of quartz and feldspar, indicating west side-up movement.

U-Pb zircon geochronology of the Western Domain granitic protoliths give ages between ca 1650-1640 Ma (Carson *et al.* 2009), which are identical to the ages of granitic magmatism and metamorphism in the Warumpi Province (Scrimgeour *et al.,* 2005), to the west of the Arunta region. This is dissimilar to the older ages in the adjacent Central Domain which are of depositional, igneous and metamorphic ages found in the Aileron Province, to the north to the Arunta region. This contrast ages, and

their similarity to the juxtaposition of the Warumpi and Aileron Provinces to the north and west, have been used to suggest that the western and Central Casey Inlier may contain a continuation of the suture, which has been proposed to separate the Aileron and Warumpi Provinces

SAMPLE DESCRIPTION

The samples were taken from the Eastern, Central and Western Domains of the Casey Inlier. The bulk of samples were taken in close proximity to a sample set taken by Carson *et al.* (2009). This was done in order to ensure that the age group identified by Carson could be targeted for subsequent Lu-Hf analysis. The locations of samples are shown in figure 3.

Eastern Domain petrological and monazite sample

NAC 2012-11- GARNET BIOTITE SCHIST

Garnets up to 1 cm are enclosed by a medium grained biotite foliation. Quartz is up to 8mm in size and has been elongate with the fabric. The sample contains deformed quartzofeldspahic segregation that is boudinaged within the foliation.

Central Domain metasediments

NAC 2011-076-QUARTZITE

Potassium feldspar elongate porphyry clasts up to 8mm (35%), subhedral quartz clasts up to 6mm (35%). Surrounded by anhedral plagioclase up to 2mm (5%). Retrogressed biotite grains fill the matrix (20%) along with muscovite (5%).

NAC 2011-079- BANDED K FELDSPAR MIGMATITE

Fine grained gneiss with slightly elongated grains of quartz grain up to 3mm and potassium feldspar up to 1mm in size, make up 60 % of the rock in bands. Platy biotite grains up to 1mm long make up 40% of the rock.

NAC 2011-081-FINE GRAINED MUSCOVITE BEARING QUARTZITE WITH FE-STAINING

Orange fine equal sized grained schist sample, dominated by quartz grains ~80% and muscovite grains (20%) and (~1%) biotite.

Central Domain granites

NAC 2011-077-AMPHIBOLE PYROXENE RICH METAGABBRO

Medium grained gabbro containing surrounded elongate crystals up to 1cm of orthopyroxene (20%), 1mm size plagioclase grains (10%) and euhedral hornblende grains up to 2mm in size (5%).

NAC 2012-18-WEAKLY GNEISSIC GRANITE

Elongate grains with the slightly linear fabric contains potassium feldspar euhedral clasts up to 5 cm in size (20%), anhedral elongate clasts of quartz up to 0.5 mm (30%) and biotite rich retrogressed matrix (50%).

NAC 2012-21- AUGEN GNEISS

Highly strained and contains elongate potassium feldspar anhedral to subhedral porphryoblasts that are up to 3 cm long (40%). Plagioclase elongate quartz clasts of

0.8mm long grains (25%) and quartz elongate sub rounded grains up to 0.6mm (25%). lasts wrapped by biotite forming less 10% of the lithology.

Central Domain petrological samples

NAC 2012-37- GARNET MUSCOVITE SCHIST

This sample is derived from a retrogression of migmatitic metasediment. It was taken from a 3m wide shear one trending in a (Figure 15a). NNW-SSE and displaying west-up shear sense.

Garnet poiquioblasts of 1cm in size has been elongate with the fabric. Biotite lenses rap the garnet (30%) with a retrogressed plagioclase matrix (60%).

NAC 2012-46- BIOTITE MYLONITE

Subvertical NNW trending shear fabric that deforms migmatised metasediments. Movement sense was west-up along a steeply plunging-lineation. Quartz clasts up to 6mm in size are elongate with the fabric. Small muscovite grains have formed veins wrapping the quartz clasts (20%). Biotite rich retrogressed mylonite (30%) and plagioclase matrix (50%).

Western Domain granites

NAC 2011-072-GRANITIC GNEISS BANDED METAGRANITE WITH 1 CM K-FELDSPAR GRAINS

Light grey granite containing sub to anhedral feldspar grains (30%) up to 1cm size that are elongate and a line with the fabric. Quartz grains (20%) are sub to anhedral and 5mm in size. The fabric is defined by biotite and elongate feldspar crystals up to 1mm making up 45% of the composition as well as muscovite (5%).

NAC 2011-073-MUSCOVITE RICH QUARTZ-FELDSPAR RICH LEUCOGRANITE

Fine grained foliated granitic gneiss predominantly anhedral quartz and K-feldspar grains (55%) and euhedral muscovite grains up to 1mm (39%). Biotite grains 1mm size is predominantly associated with muscovite rich areas.

NAC 2011-074- PORPHYRITIC BIOTITE RICH FOLIATED GRANITE WITH 2CM LONG K-FELDSPAR

Porphyritic biotite rich foliated granite with 2cm long K-feldspar aligned with the fabric (20%). Quartz has a similar orientation and shape to the feldspar with 8mm size grains (10%). The larger phenocrysts are surrounded by a matrix of plagioclase which are up to 6mm in size (35%), K feldspar making up to 2cm (30%) and biotite grains up to 1mm long (5%).

PETROLOGICAL DESCRIPTIONS

SAMPLE NAC 2012-11- GARNET BIOTITE SCHIST

In thin section garnet, biotite, sillimanite, quartz, plagioclase feldspar, muscovite, hornblende, and monazite can be seen. Sub rounded to slightly elongate garnet porphyroblasts (up to 6m in diameter) contain small inclusions of anhedral biotite, quartz, and euhedral hornblende has formed on the margin of garnets (Figure 9a), replacing the garnet grain. Coarse biotite grains dominated fabric wraps the garnets and dominates the matrix. The lenses contain predominantly biotite and small amounts muscovite and sillimanite, in the retrogressed plagioclase porphryoblasts (up to 2mm in diameter). The sillimanite in the biotite has formed vines which have formed clusters (Figure 9b). Anhedral quartz grains are predominantly associated with the plagioclase

and form veins aligned with the fabric, with anhedral and euhedral tourmaline small 0.01 mm grains (Figure 9c).

SAMPLE NAC 2012-37- GARNET MUSCOVITE SCHIST

This sample contains garnet, plagioclase feldspar, biotite, quartz, muscovite, apatite and monazite. Anhedral garnet porphryoblasts (up to 5mm) replaced with quartz, sillimanite and biotite in a retrogressing plagioclase matrix which is breaking down into sillimanite and quartz (Figure 9d). The fabric that wraps the garnet grains is predominantly fine grained muscovite and quartz. This is intermixed with elongate biotite gains, which create lenses (up to 7mm) within the matrix (Figure 9e). Monazites are anhedral with grains sizes up to 50µm and which are altered by the feldspar matrix and have developed apatite rich halos (Figure 9f).

SAMPLE NAC 2012-46- BIOTITE MYLONITE

This sample contains plagioclase feldspar, quartz, biotite, muscovite and garnet. The retrogresses plagioclase feldspar porphyroblasts (up to 1mm) are euhedral in shape and are being replaced by predominantly quartz clasts and anhedral biotite grains. There are lenses of anhedral biotite grains (up to 0.08mm) with semi-rounded, small anhedral grains of quartz grains (up to 0.3 mm) anhedral muscovite grains (up to 0.02mm) within the matrix. (Figure 9g) Monazites are anhedral with grains sizes up to 50µm and which are altered by the feldspar matrix and have developed apatite rich halos (Figure 9h).

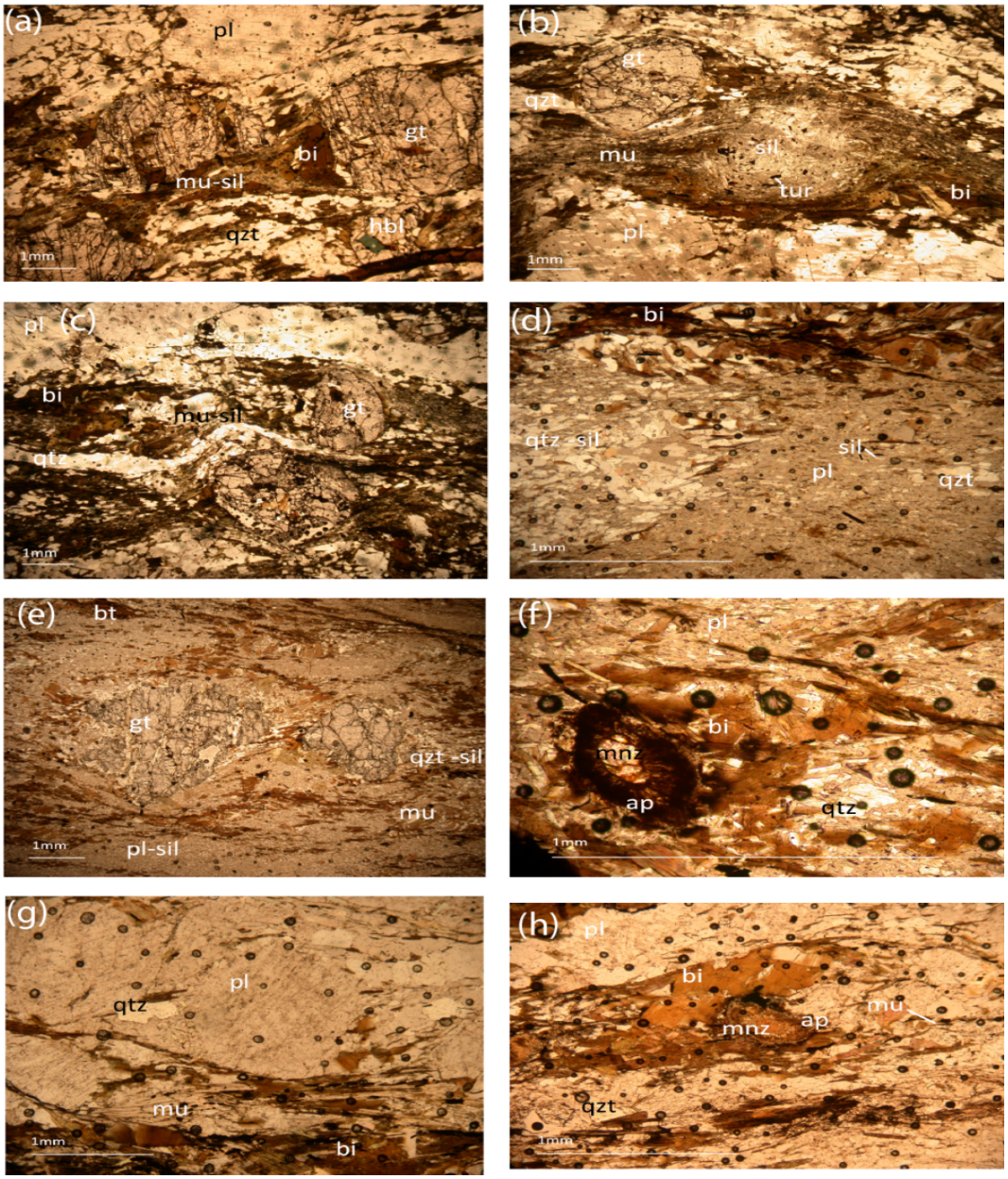

Figure 9: Mineral abbreviations used: gt= garnet, bi= biotite, sil=sillimanite, qtz= quartz, pl= plagioclase feldspar, mu= muscovite, hbl=hornblende, ap= apatite tur=tourmaline and mnz=monazite. a) Photomicrographs of sample NAC 2012-11 elongate garnet porphyroblasts with inclusions of biotite, plagioclase euhedral hornblende on the margin of garnets. Biotite, muscovite and sillimanite wrap the garnets and lenses of biotite retrogresses plagioclase and quarts clasts surrounding them.
b) Photomicrographs of sample NAC 2012-11 showing a sillimanite cluster of grains in the lens biotite muscovite rich plagioclase matrix c) Photomicrographs of sample NAC 2012-11showes veins of quart elongate with the fabric d) Photomicrographs of sample NAC 2012-37 showing a garnet replaced by quart and sillimanite in a sillimanite plagioclase matrix e) Photomicrographs of sample NAC 2012-37 shows a garnet that is being wrapped by muscovite and quartz and biotite lenses in eth retrogressing plagioclase matrix breaking down to sillimanite. f) Photomicrographs of sample NAC 2012-37 shows an appetite alteration halo around a monazite grain in a retrogressed plagioclase and sillimanite matrix with zones of quartz and biotite. g) Photomicrographs of sample NAC 2012-46 shows retrogressed plagioclase with a biotite muscovite domain and quartz inclusions h) Photomicrographs of sample NAC 2012-46 shows an alteration halo of apatite around a monazite grain with a retrogressed plagioclase with quartz and sillimanite matrix with lenses of biotite.

METHODS

U-Pb LA-ICP-MS geochronology

Single-grain U–Pb zircon dating was undertaken using Laser Ablation – Inductively Coupled Plasma Mass Spectrometry LA-ICPMS at the University of Adelaide following a similar method to Payne *et al.* (2010). Zircon grains were extracted from the rock samples using routine crushing, sieving, panning, Frantz Isodynamic separation and heavy-liquid separation. The zircons were then handpicked and mounted in a 2.5cm diameter circular epoxy grain. Each mount was polished to expose the approximate centre of the zircon grain. The mounted zircon grains were imaged using backscatter electron (BSE) and cathodoluminescence (CL) imaging on a Phillips XL-20 Scanning Electron Microscope (SEM).

U–Pb isotopic analyses was done using the New Wave 213 nm Nd-YAG laser coupled to an Agilent 7500cs ICP-MS at the University of Adelaide. The ablation was performed in a He atmosphere with a 30μm spot size, repetition rate of 5Hz and a laser intensity of 9-10 J/cm^2. The total analysis time is 120 seconds which consists of 30 seconds of background measurements, 10 s of laser stabilisation with the shutter closed and 80 s of sample ablation. The isotopes measured were ^{204}Pb, ^{206}Pb, ^{207}Pb and ^{238}U for 10, 15, 30 and 15 ms, respectively.

Corrections were made for U-Pb mass bias and instrument drift with the external zircon standard GJ (TIMS normalisation data: ^{207}Pb/^{206}Pb age= 607.7 ± 4.3 Ma; ^{206}Pb/^{238}U age= 600.7 ± 1.1 Ma; ^{207}Pb/^{235}U age= 602.0 +/- 1.0 Ma: (Jackson *et al.* 2004). The Plešovice standard was also run to monitor the accuracy of the method (ID-TIMS

normalisation data: $^{207}Pb/^{206}Pb$ age= 337.13 ±□ 0.37 Ma: (Slama *et al.* 2008b) . The data was processed using the real-time processing program 'Glitter', developed at Macquarie University, Sydney (Jackson *et al.* 2004). Common Pb anomalous was discarded. Isoplot v4.11 (Ludwig 2003) is used to calculate conventional concordia and weighted average plots were created. Concordancy of the data was calculated using the ratio of $2^{06}Pb/^{238}U$ /$^{207}Pb/^{206}Pb$ ages. All ages are reported at 1δ uncertainty. The standard age obtained during this study was GJ $^{207}Pb/^{206}Pb$= 610 ± 3.8 Ma (n=329, MSWD=0.44), $^{206}Pb/^{238}U$= 601.05 ± 0.89 Ma (n=327, MSWD=1.07) and $^{207}Pb/^{235}Pb$= 602.69 ± 0.91 Ma (n=313,MSWD=0.58) and Plešovice are $^{207}Pb/^{206}Pb$= 345.6.3 ± 6.3 Ma (n=114, MSWD=0.57), $^{206}Pb/^{238}U$= 336.5 ± 1.1Ma (n=115, MSWD=1.9) and $^{207}Pb/^{235}Pb$= 337.9 ± 1.1 Ma (n=113, MSWD=1.4).

Monazite U-Pb dating was done on in-situ monazite grains within thin sections. Thin sections and monazites were imaged using a Phillips XL40 Scanning Electron Microscope (SEM) on backscatter electron (BSE) settings to locate the monazites. U-Pb isotopic analyse was undertaken using a New Wave 213 nm Nd-YAG laser together with an Agilent 7500cs ICP-MS at the University of Adelaide. The ablations were performed in a helium atmosphere, with a 15 μm beam diameter on the sample surface, with a laser intensity of 9^{-10} J/cm2 at a repetition rate of 5 Hz. Total acquisition time for each sample was 90 s, consisting of 20 s of background measurement, 10 s of shutter closed laser firing to allow for beam stabilisation and 60 s of sample ablation. Isotopic masses were measured from ^{204}Pb, ^{206}Pb, ^{207}Pb and ^{238}U for 10 ms, 15 ms, 30 ms and 15 ms respectively (Payne *et al.* 2008). GLITTER was used to process the raw LA-ICP-MS data which is a reduction program developed at Macquarie University.

Sydney (Griffin *et al.* 2008).

Corrections were made using the monazite standard MAdel (TIMS normalisation data: $^{207}Pb/^{206}Pb$ age= 491.0± 2.7 Ma; $^{206}Pb/^{238}U$ age= 518.37±0.99 Ma; $^{207}Pb/^{235}U$ age= 513.13± 0.19 Ma: Payne *et al.* 2008; updated with additional TIMS data), the external monazite standard 44069 was also used (TIMS normalisation data: $^{206}Pb/^{238}U$ = 426 ±3 Ma: Aleinikoff *et al.* 2006). Data accuracy and correction was monitored by repeated analysis of the in-house monazite standard 94-222/Bruna NW (*c.* 450 Ma)(Payne *et al.* 2008). Throughout this study, the weighted averages obtained for 222 are $^{207}Pb/^{206}Pb$= 455 ± 16 Ma (n=23, MSWD=1.2), $^{206}Pb/^{238}U$= 456.3 ± 5.4 Ma (n=22, MSWD=3.7) and $^{207}Pb/^{235}Pb$= 453.2±5.9 Ma (n=22, MSWD=4.3), Madel are $^{207}Pb/^{206}Pb$= 489 ±10 Ma (n=39, MSWD=1.12), $^{206}Pb/^{238}U$= 519 ±3 Ma (n=37, MSWD=1.6) and $^{207}Pb/^{235}Pb$= 513±2.6 Ma (n=36, MSWD=1.3) and 44069 are $^{207}Pb/^{206}Pb$= 395±21 Ma (n=7, MSWD=0.73), $^{206}Pb/^{238}U$= 423.8±6.3 Ma (n=7, MSWD=1.4) and $^{207}Pb/^{235}Pb$= 418±6.6 Ma (n=7, MSWD=1.7).

Lu-Hf LA-MC-ICP-MS zircon isotope analysis

Thermo-Scientific Neptune Multi Collector ICP-MS equipped with Faraday detectors and $10^{-11}\Omega$ amplifiers was used to make measurements. Analyses where made using a dynamic measurement routine with: Ten 0.524 s integrations on ^{171}Yb, ^{173}Yb, ^{175}Lu, ^{176}Hf(+Lu+Yb), ^{177}Hf, ^{178}Hf, ^{179}Hf and ^{180}Hf; one 0.524 s integration on ^{160}Gd, ^{163}Dy, ^{164}Dy, ^{165}Ho, ^{166}Er, ^{167}Er, ^{168}Er, ^{170}Yb and ^{171}Yb, and one 0.524 second integration of Hf oxides with masses ranging from 187 to 196 amu. Between each mass change there was an idle time of 1.5 seconds which allow for magnet settling and to negate any

potential effects of signal decay. 15 repetitions of this measurement cycle were made to provide a total maximum measurement time of 3.75 minutes including an off-peak baseline measurement. This measurement routine has been used to allow the monitoring of oxide formation rates and REE content with in the zircon and provide an option to correct for REE-oxide interferences if necessary.

An exponential fractionation law stable $^{179}Hf/^{177}Hf$ ratio of 0.7325 was used to correct for Hf mass bias. Yb and Lu isobaric interferences on ^{176}Hf were corrected for following the methods of Woodhead *et al.* (2004). ^{176}Yb interference on ^{176}Hf was corrected for by measurement of Yb fractionation using the measured $^{171}Yb/^{173}Yb$ ratio with the Yb isotopic values from(Segal *et al.* 2003). The Lu isobaric interference on ^{176}Hf was corrected using a $^{176}Lu/^{175}Lu$ ratio of 0.02655 (Vervoort *et al.* 2004), assuming the same mass bias behaviour of as Yb. Set up of the MC-ICP-MS prior to laser ablation setup was done using analysis of JMC475 Hf solution. Accuracy of technique used for zircon analysis was determined by monitoring the use a combination of the Plešovice and Mudtank standards. The average value for Plešovice for the analytical session was 0.2824678±0.0000081 (2σ, n=5). This compares to the published value of 0.282482 ± 0.000013 (2σ) (Slama *et al.* 2008a, Slama *et al.* 2008b). The average value for Mudtank for the analytical session was 0.2825005±0.0000051 (2σ, n=11).

TDM and TDM crustal age was calculated using the ^{176}Lu decay constant (Scherer *et al.* 2001). The average crustal composition of $^{176}Lu/^{177}Hf$=0.015 was used to calculate TDM crustal age following the methods of Griffin et al. (2002).

RESULTS

U-Pb zircon LA-ICP-MS geochronology

The fully tabulated results are shown in appendix a, representative cathodoluminescence (CL) images of each sample in figure 10, probability density plots for metasedimentary data in figure 11 and concordia data plots for the igneous samples in figure 12.

Central domain metasediments

SAMPLE NAC 2011-076

Forty four analyses were obtained from 44 oscillatory zoned zircons grains, with distinctive cores and rims which both were analysed (Figure 10a). Seventeen analyses were rejected due to falling outside of 90-110% concordance. U-Pb concordia plot were used to plot these analysis, which revealed four populations (Figure 11a). The $^{207}Pb/^{206}Pb$ ages oldest grains are ca 2517 and 2151 Ma. The weighted average age of the second oldest population is a mean of 2517±25 Ma (n=4, MSWD=0.54) Second oldest population had only one grain that had a weighted average age of ca 2151 Ma. The second youngest and youngest population have a weighted average of $^{207}Pb/^{206}Pb$ age 1909±13 Ma (n=12, MSWD=0.51) and 1886±17 Ma (n=13, MSWD=0.30) (Figure 11a).

SAMPLE NAC 2011-079

Forty analyses were obtained from 39 oscillatory zircon grains, with dominating rims compared to cores, which both were analysed (Figure 10b). Fourteen analyses were rejected due to falling outside of 90-110% concordance. U-Pb concordia plot were used to plot these analysis, which revealed five populations (Figure 11b). The $^{207}Pb/^{206}Pb$

ages of the oldest grains are ca 2590, 2511 and 2246 Ma. The second youngest and youngest population have a weighted average of $^{207}Pb/^{206}Pb$ age 1970±23Ma (n=8, MSWD=0.51) and 1882±18 Ma (n=9, MSWD=0.30) (Figure 11b).

SAMPLE NAC 2011-081

Eighty five analyses were obtained from 85 rounded oscillatory zoned zircon grains with rims and core were analysed (Figure 10c). Four analyses were rejected due to falling outside of 90-110% concordance. U-Pb concordia plot were used to plot these analysis, which revealed three populations (Figure 11c). The $^{207}Pb/^{206}Pb$ weighted average age of the oldest population is a mean of 1735±14 Ma (N=18, MSWD=0.74). Second oldest and youngest population has a weighted average age of 1577±17 Ma (n=15, MSWD= 0.93) and 1330±28 Ma (n=6, MSWD= 0.4) (Figure 11c).

Central Domain granites

SAMPLE NAC 2011-077

Sixty one analyses were obtained from 61 oscillatory sector zircon grains, with rims and cores which were analysed (Figure 10d). One analysis was rejected due to falling outside of 90-110% concordance and three have been removed due to being dark grains. U-Pb concordia plot were used to plot these analysis, which revealed one population data set (Figure 12a). The $^{207}Pb/^{206}Pb$ weighted average age population is a mean of 1774±8 Ma (n=57, MSWD=0.60) (Figure 12a).

SAMPLE NAC 2012-18

Seventy two analyses were obtained from 72 oscillatory zircon grains with rims and cores were analysed (Figure 10e). Forty seven analyses were rejected due to falling

outside of 90-110% concordance and two have been removed are inherited grains with the ages of ca 1876.8 and 1877.8 Ma. U-Pb concordia plot were used to plot these analysis (Figure 12b). The $^{207}Pb/^{206}Pb$ weighted average age of the youngest population which only contains rims has a mean of 1756±13 Ma (n=14, MSWD=0.64) and the older populations which contains rims and cores, with a $^{207}Pb/^{206}Pb$ weighted average population ages has a mean of 1813±17 Ma (n=9, MSWD=0.6) (Figure 12b).

SAMPLE NAC 2012-21

Seventy seven analyses were obtained from 74 oscillatory broken zircon grains, with both rims and cores were analysed (Figure 10f). Forty-two analyses were rejected due to falling outside of 90-110% concordance and one for having high ^{207}Pb. U-Pb concordia plot were used to plot these analysis, which revealed four population data set (Figure 12c). The $^{207}Pb/^{206}Pb$ weighted average age of the youngest population is a mean of 1729±17 Ma (n=9, MSWD=0.34). The oldest population has a weighted average of $^{207}Pb/^{206}Pb$ age 1779±10 Ma (n=24, MSWD=0.67) which concludes the one age peak. The older population contains all the cores analysed in the sample (Figure 12c).

Western domain granites

SAMPLE NAC 2011-072

Sixty analyses were obtained from 51 zoned zircons grains with smaller cores than rims, which were both, were used for analysis (Figure 10g). Twenty seven were rejected due to falling outside of 90-110% concordance and five for having migmitic cores. U-Pb concordia plot were used to plot these analysis, which revealed one population data set

(Figure 12d). The $^{207}Pb/^{206}Pb$ weighted average age population is a mean of 1660±19 Ma (n=24, MSWD=0.29) (Figure 12d).

SAMPLE NAC 2011-073

Eighty two analyses were obtained from 79 oscillatory zoned zircons grains with smaller cores than rims, which both were analysis (Figure 10h). Forty nine analyses were rejected due to falling outside of 90-110% concordance and three were not used in calculating the weighted average due to high common lead. U-Pb concordia plot were used to plot these analysis, which revealed one population data set (Figure 12e). The $^{207}Pb/^{206}Pb$ weighted average age population is a mean of 1660±9 Ma (n=33, MSWD=0.66) (Figure 12e).

SAMPLE NAC 2011-074

Twenty seven analyses were obtained from 26 oscillatory zoned zircons grains with smaller cores than rims, which both were analysed (Figure 10i). Two analyses were rejected due to falling outside of 90-110% concordance and three have been removed due to having high common lead. U-Pb concordia plot were used to plot these analysis, which revealed one population data set (Figure 12f). The $^{207}Pb/^{206}Pb$ weighted average age population is a mean of 1652±9 Ma (n=20, MSWD=0.25) (Figure 12f).

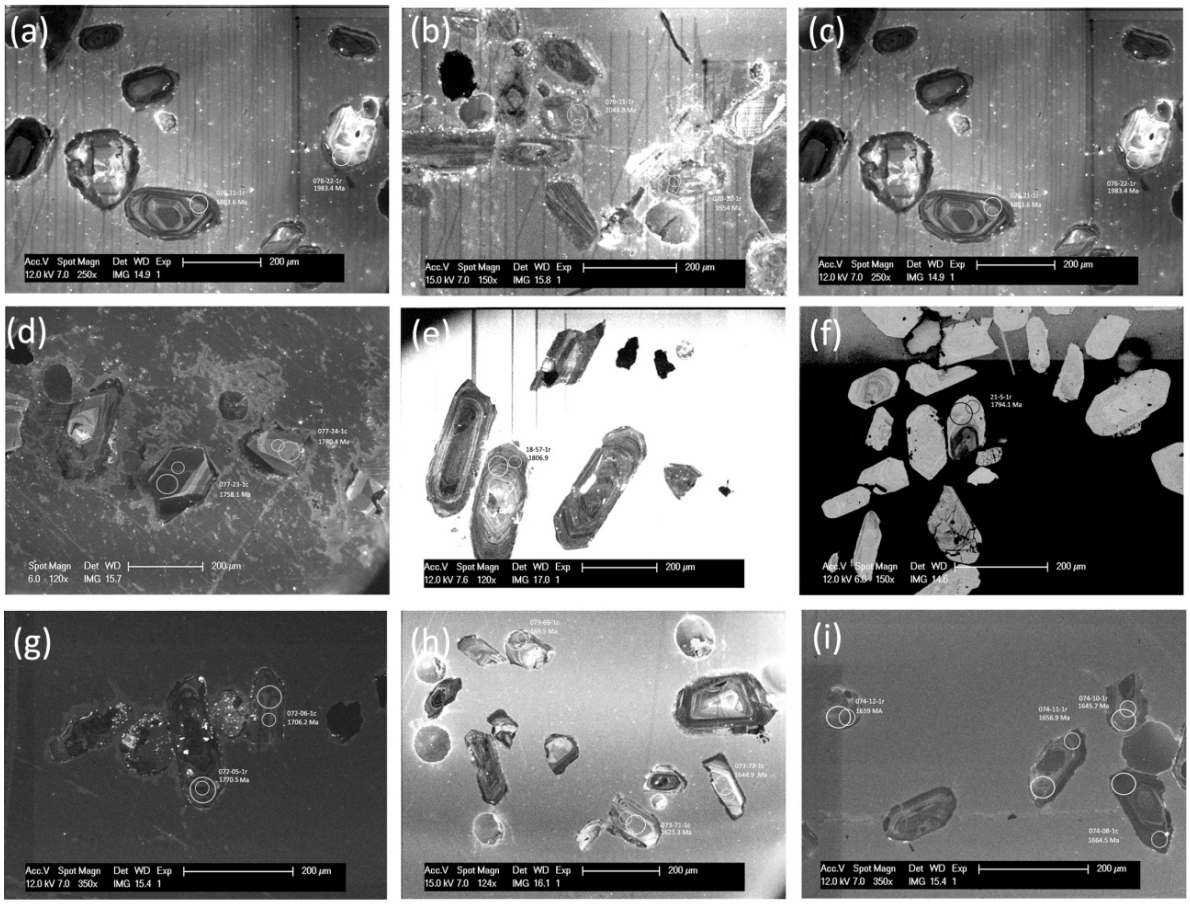

Figure 10: Cathodoluminescence images of representative zircon grains for each analysed sample. Grains are labelled with their sample number, U-Pb laser analysis spot and age (small white circle) with the age of location and Lu-Hf. Image a) NAC 2011-076, b) NAC 2011-079, c) NAC 2011-081, d) NAC 2011-077, e) NAC 2012-18, f) NAC 2012-21, g) NAC 2011-072, h) NAC 2011-073 and i) NAC 2011-73

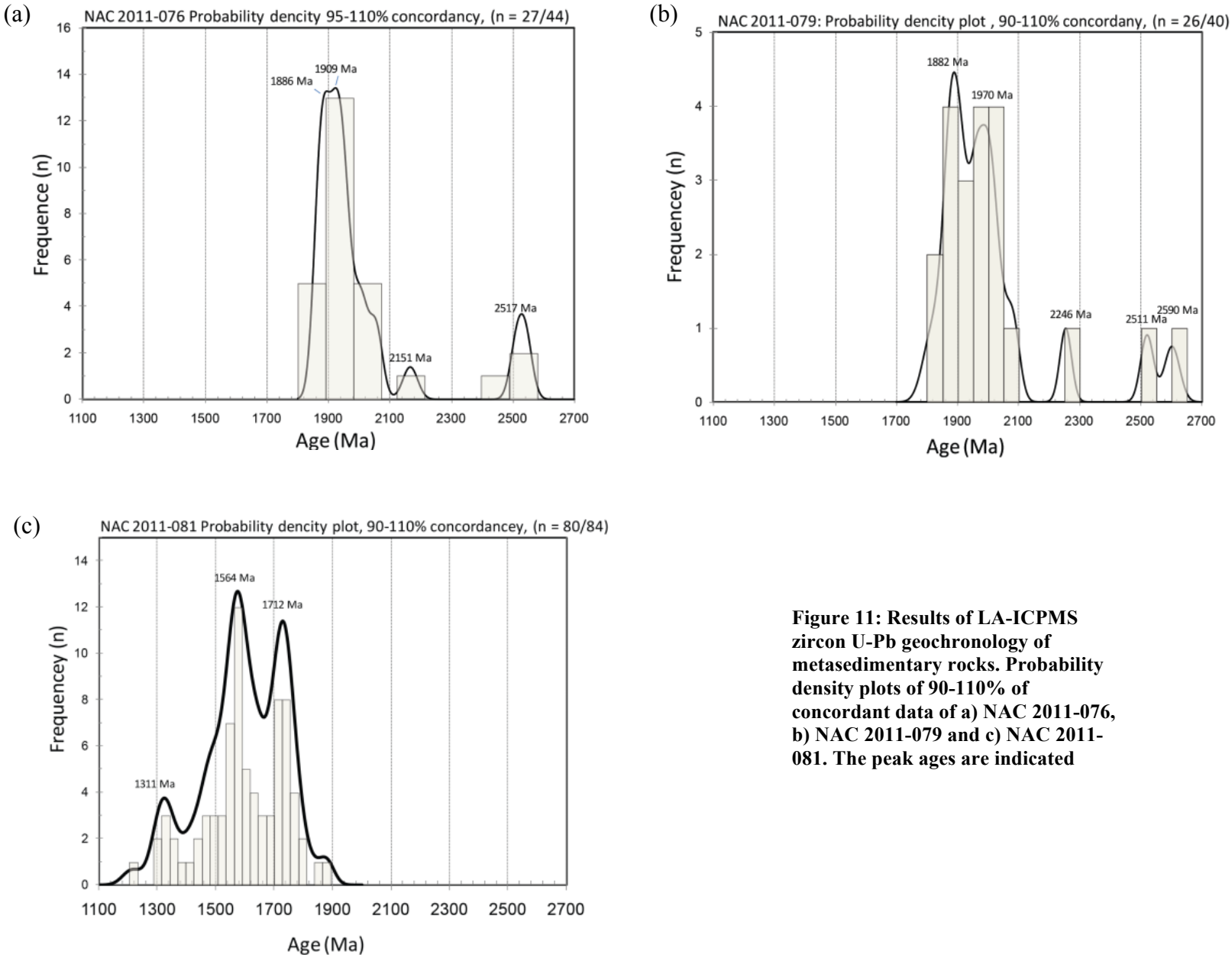

Figure 11: Results of LA-ICPMS zircon U-Pb geochronology of metasedimentary rocks. Probability density plots of 90-110% of concordant data of a) NAC 2011-076, b) NAC 2011-079 and c) NAC 2011-081. The peak ages are indicated

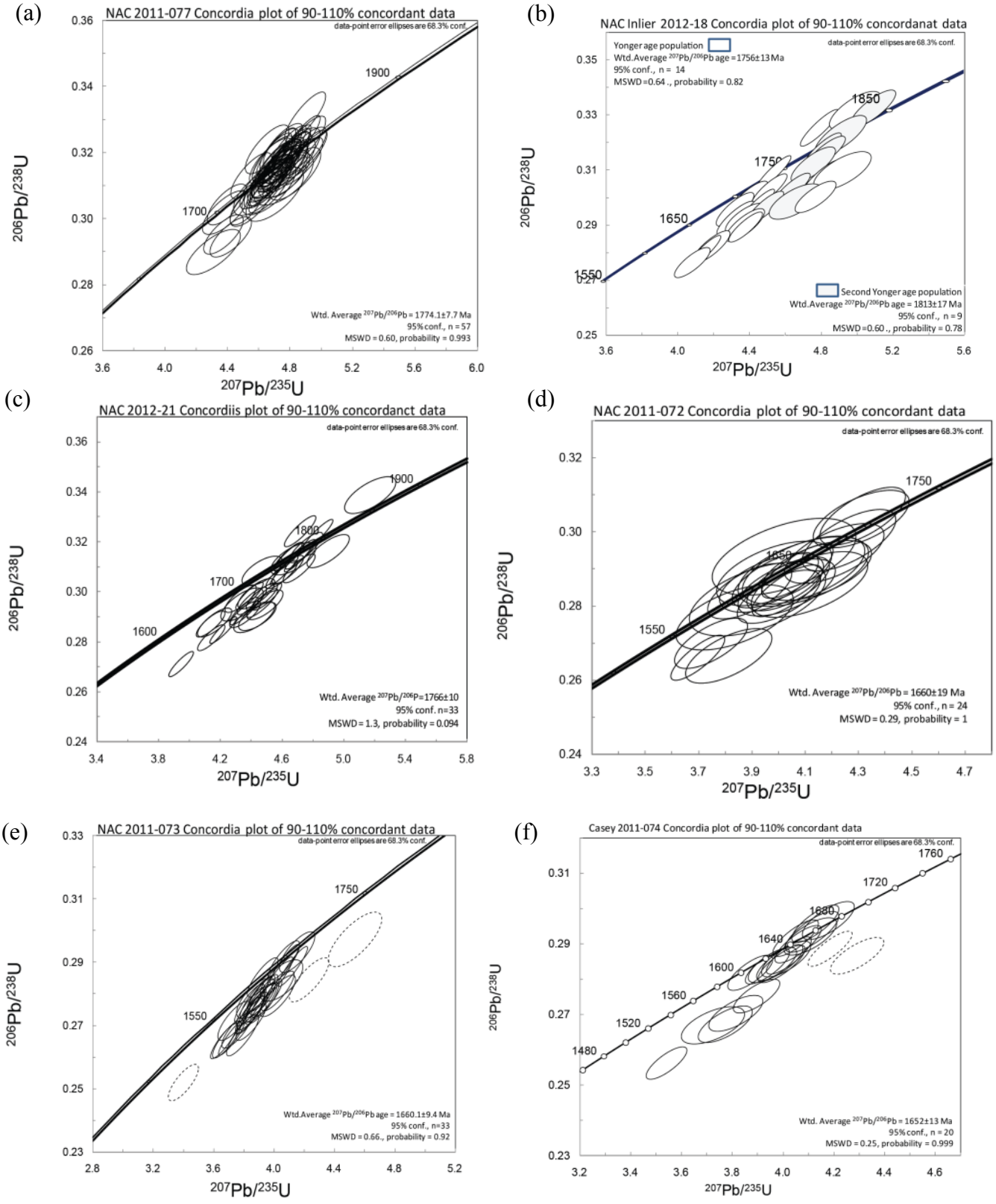

Figure 12: Results of LA-ICPMS zircon U-Pb geochronology of igneous lithologies. Concordia plots for: a) NAC 2011-077, b) NAC 2012-18, c) NAC 2012-21 from the central domain and d) NAC 2011-072, e) NAC 2012-073 and f) NAC 2012-074of the western domain. All ages are weighted averages of data within 90-110% concordancy. Soiled ellipses are data used in age calculations and dotted ellipses represent data points discarded from age calculations and dotted ellipses represent data points from discarded from age calculations due to high ^{204}Pb and where not used in the calculation of the weighted average age. For sample b) NAC 2012-18 the shaded ellipses represent the older population obtained from analyses of zircon cores and rims with the unshaded ellipses represent younger population obtained from rim analysis. These two age packages were identified and determined using Isoplot v4.11

Monazite analysis

U-Pb monazite data results are provided in supplementary appendix b. Up-Right NNW-SSE trending fabric that dominates the eastern domain and similar to the foliation that reworks the granulites in the central domain monazite geochronology was undertaken on sample, NAC 2012-11 containing the pervasive fabric within the area. In-situ monazite geochronology was conducted on grains in thin section allowing monazites with constrained microstructural locations, where the monazite aligned with the fabric (Kelsey *et al.* 2007, Payne *et al.* 2008) (Figure 13a) Sample NAC 2012-11 twenty four analysis were done on 20 grains located in the matrix (Fig 14a) Five were rejected as they fell outside the 95-105% concordance range. A concordia plot was calculated and yield an age of 1732±11 Ma (n= 15, MSWD= 0.67) (Figure 13b)

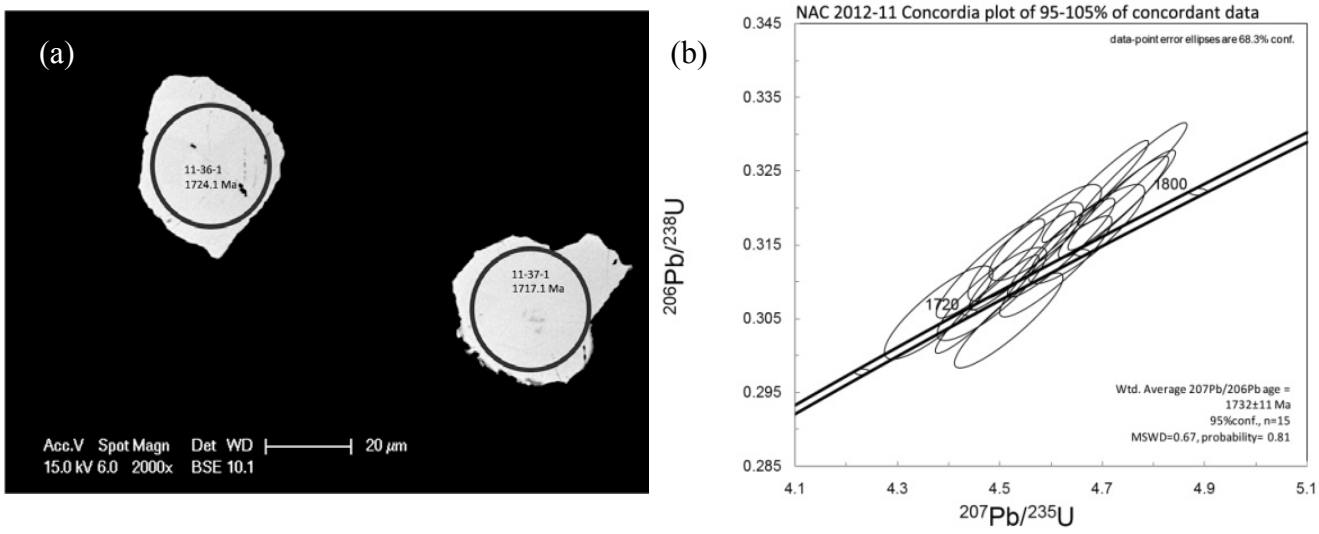

Figure 13: Results of LA-ICPMS monazite U-Pb geochronology of sample NAC 2012-11, with CL images of selected grains showing age and spot of analysis indicated in image a. Twenty four analysis were done on 20 grains located in the matrix. Nine analyses were rejected as they fell outside the 95-105% concordance range. A concordia plot was calculated and yield an age of 1732±11 Ma (n=15, MSWD= 0.67) indicated in image b.

Zircon Lu-Hf isotopic data results

Zircon Hf isotopic results are provided in figure 14a and 14b and the fully tabulated results are shown in appendix c. Data were obtained from three metasedimentary samples; NAC 2011-076, NAC 2011-79 and NAC 2011-081; and from six metaigneous samples; NAC 2011-077, NAC 2012-18, NAC 2012-21 NAC 2011-072, NAC 2011-073 and NAC 2011-074.

Representative grains chosen from detrital populations in the Central and Eastern Domains samples, NAC 2011-076 and NAC 2011-079 at ca 1880, 1910, 1970, 2150, 2250, 2510, 2520 and 2590 Ma. Present-day Hf isotopic compositions range from 0.281190 to 0.28145 for the grains, corresponding to predominantly evolved epsilon hafnium (ε_{Hf}) values that range from -9.7 to +8.8 (Figure 14a, b). The εHf values of the detrital zircon peaks are variable. The $^{207}Pb/^{206}Pb$ analysis of the eldest four zircon grains crystallisation ages are ca 2303, 2511, 2543 and 2601 Ma, and yield ε_{Hf} values between 2.5 and 8.8 (T_{DM} of 2.3, 2.7, 2.75 and 2.8 Ga, respectively). Two grains at ca 2100 and ca 2166 Ma yield ε_{Hf} values of 1.5 and 5.4 (T_{DM} of 2.41 and 2.32 Ga, respectively). Zircon grains aged between ca 2055- 2008 Ma record highly variable εHf values between -2 and +3.5 (T_{DM} of 2.23- 2.55 Ga), grains ranging over peak ca1909-1970 Ma yield εHf values between -4.4 and 1.7 (T_{DM} between 2.24 and 2.9 Ga). Zircon grains between ca1882 -1886 Ma ranging over the grain analysis from ca1849 to 1892 Ma yields zircons that record ε_{Hf} values between -7.9 and +1.12 (T_{DM} between 2.31 and 2.57 Ga). Zircon grains in the same age range ca172-1779 Ma encompassed the grain analysis ca 1705-1815 Ma yield ε_{Hf} values between -9.7 and 3.22 (T_{DM} between 2.25 and 2.62 Ga) (Figure 14a).

The metasedimentary rock cover sequence that overlays the Central and Eastern Domains, NAC 2011-081 has zircon grains that have peaks of ca 1311.95, 1544.4 and 1712.17 Ma. The grain from the peak ca 1311 Ma yields ε_{Hf} values between 3.3 and 6.4 (T_{DM} between 1.58 and 1.84 Ga). The grain from the peak ca 1544.4 Ma yields ε_{Hf} values between -14.6 and 6.5 (T_{DM} between 1.72 and 2.62 Ga). The grain from the peak ca 1712.17 Ma yields εHf values between –4.9 and 6.2 (T_{DM} between 1.9 and 2.31 Ga) (Figure 14a).

Igneous zircon grains in the Eastern and Central Domain sample NAC 2011-077, NAC 2012-18 and NAC 2012-21 are between ca 1705.9- 2053.5 Ma yielding a U-Pb mean ages of 1774± 7 , 1756 ±13 and 1766±1 Ma present day Hf isotopic compositions of 0.281568 to 0.281759. Corresponding ε_{Hf} values range from -4.4 to 3.2, and T_{DM} varied between 2.08 and 2.36 Ga (Figure 15a and 15b).

Sample NAC 2011-077 zircon grains are between ca 1709.9 -1812.8 Ma (mean=1774.1±7.7 Ma) and yield consistent ε_{Hf} values -4.38 to -1.82 (T_{DM} between 2.27 and 2.35 Ga) (Figure 14a).. NAC 2012-18 zircon grains yield a U-Pb ages between ca 1791.5-18176.8 Ma (mean= 1756±13 Ma), yielding ε_{Hf} values between -1.46 and 1.23 (T_{DM} between 2.22 and 2.26 Ga) (Figure 14a).. NAC 2012-21 has zircon grain between ca 1705.9 -2053.5 Ma (mean= 1766±1 Ma), yielding ε_{Hf} values between -3.46 and 3.22 (T_{DM} between 2.08-2.36 Ga) (Figure 14a).

Igneous zircon grain in the Western Domain samples NAC 2011-072, NAC 2011-073 and NAC 2011-074 have U-Pb ages between 1652± 13 Ma and 1670±18 Ma, with a

present day Hf isotopic of 0.281734 to 0.281602, which has a corresponding ε_{Hf} values range from 0.63 to -4.76, and T_{DM} varied between 2.09 and 2.27 Ga (Figure 14a, b).

Sample NAC 2011-072 zircon grains are between ca 1603-1770 Ma (mean=1670±18 Ma) and yield consistent ε_{Hf} values -0.4 to -4.14 (T_{DM} between 2.18 and 2.27 Ga) (Figure 14a).. NAC 2011-073 zircon grains yield a U-Pb ages between ca 1585 Ma and 1810 Ma (mean= 1660± 9 Ma), yielding ε_{Hf} values between -4.14 and 0.63 (T_{DM} between 2.09 and 2.25 Ga) (Figure 14a).. NAC 2011-074 has zircon grain between ca 1629 -1776 Ma (mean= 1652± 13 Ma), yielding ε_{Hf} values between -4.76 and -1.34 (T_{DM} between 2.2-2.27 Ga) (Figure 14a).

(a)

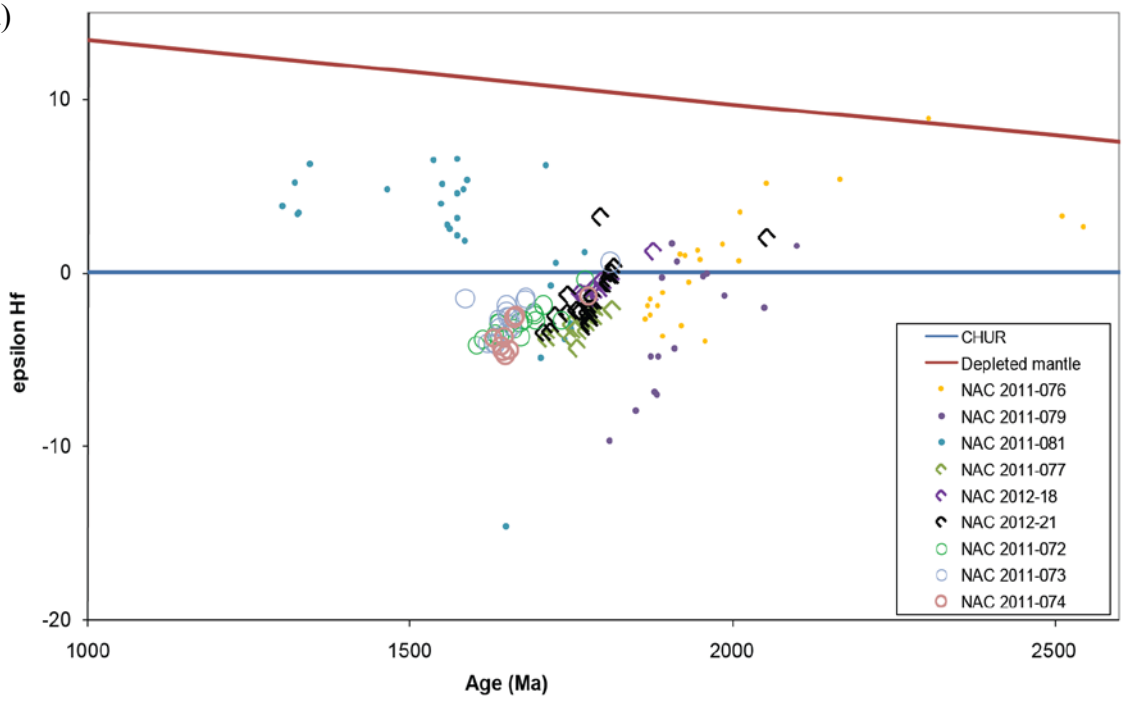

(b)

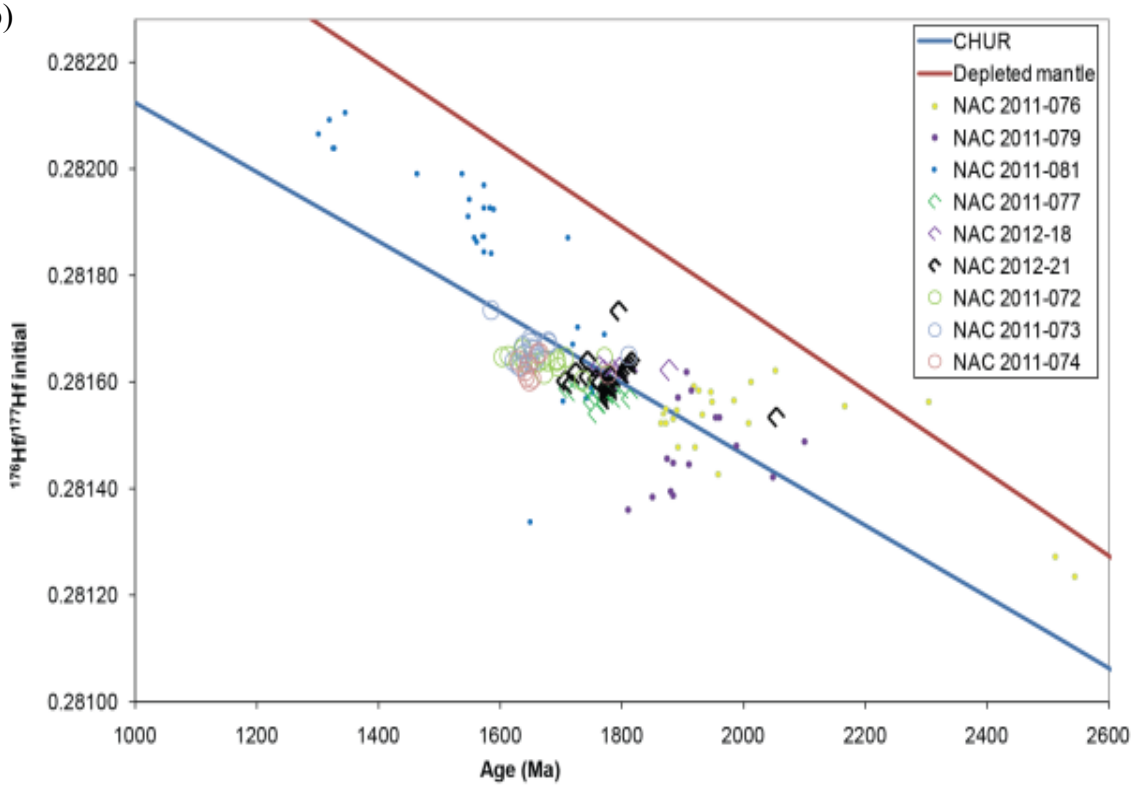

ıre 14: Plot of epsilon Hf against zircon grains $^{207}Pb/^{206}$ Pb age in a, and in b the $^{176}Hf/^{177}Hf$ ınst zircon grains $^{207}Pb/^{206}$ Pb age. The blue line indicates CHUR and the red indicates the depleted mantel. Samples are indicated by their denotation in the ledged.

DISCUSSION

The Casey Inlier has been interpreted to preserve a ca 1640 Ma suture (Close *et al.* 2004) between the ca 1780-1830 Ma Aileron Province, thought to be represented by the Eastern and Central Domains of the Casey Inlier, and the ca 1640-1690 Ma Warumpi Province, the western side of the Casey Inlier (Scrimgeour *et al.* 2005). The collected results and observations in this study are able to assist in determining the palaeogeography of the region and in the interpretation of the bulk crustal composition on either side of the proposed boundary. The collection of results has been summarised in and clearly indicates that two magmatic ages and which correspond to the spatially to the locations to the rocks that are found either side of the proposed NS-oriented suture (Table 2).

Interpretation of U-Pb zircon age from basement metasedimentary units

The detrital zircon age spectrums of samples NAC 2012-076 and NAC 2012-079 have ages that range between ca 1882 -2590 Ma. These both reflect youngest population peaks at ca 1886 -1882 Ma respectively and tail off in to a cluster at ca2150 -2517 Ma, which is common for NAC detrital samples (Carson *et al.* 2009) (Table 2, Figure 11a ,b). These samples were taken from concentric oscillatory zoned magmatic rims, and rims and cores respectively (Figure 10a,b). These samples indicate magmatic events that are older than the Aileron Province outlining the maximum deposition age of the Aileron Provence. These age distributions are comparable with the Lander Rock Formation (Claoué-Long *et al.* 2008), which covers most of the Arunta Region (Claoué-Long *et al.* 2008)

The detrital sample NAC-2011-081 which is the cover sequence covers the Central and Eastern Domains has detrital zircon ages ranging from ca 1311- 1712 Ma, with peaks at ca 1311, 1564 and 1712 Ma. The peak at ca1311-1564 Ma are similar to ages found in the Musgrave's located the south of the Casey Inlier, and this seems a likely source or the younger zircons (Wade *et al.* 2008, Kirkland *et al.* 2012). The peak at ca1712 Ma found in the cover does not correspond to the known ages of the Musgrave's, which is from magmatic rims and cores could be inheritance mixed in from the Aileron Province where it was deposited (Figure 11c). This constrains the Musgrave Province to being proximal to the Arunta region prior to the ca 1300Ma.

U-Pb zircon ages from granitic rocks

The magmatic rocks in the Eastern and Central Domain the Casey Inlier range between ca 1756-1776 Ma are represented by NAC 2011-077, NAC 2012-18 and NAC 2012-21. The ages are indicated in table 2. The weighted average zircon ages of NAC 2011-077 is 1774±7.7 Ma. This sample is an amphibole-pyroxene-rich metagabbro that has characteristic broad oscillatory and common sector zoned zoning zircons. Sample NAC 2021-18 and NAC 2012-21 have oscillatory zoned zircons with rims and cores. There magmatic ages correspond to the range of magmatic ages that define the Aileron Province in the west of the Arunta region.

The Western Casey Inlier has ages obtained from granites that range between ca1652-1670 Ma, which are slightly older than the comparable samples analysed by Carson *et al.* (2009). The ages are younger than the magmatic ages in the Central Casey Inlier. There magmatic age dose correspond to the range of magmatic ages that define the Warumpi Province in the west of the Arunta region.

Table 2: Summary of U-Pb ages.

		Sample Type	Easting And Nothings	U-Pb isotopic ages			Inheritance
East and central Casey Inlier	NAC 2011-076	Metapelite	0540990 7333247				1886.85 Ma, (n=8) 1909.8 Ma, (n=11) 2151.9 Ma, (n=1) 2517.3 Ma (n=2)
	NAC 2011-077	Amphibole pyroxene rich metagabbro	0540797 7332235			1774.1±7.7Ma (n=57)	
	NAC 2011-079	Biotite K feldspar Migmatite	0537521 7332366				1882 Ma, (n=4) 1970 Ma, (n=8) 2246 Ma, (n=1) 2500 Ma, (n=1) 2511 Ma (n=1)
	NAC 2012-18	Weakly gneissic granite	0538943 7336103			1756±13 Ma (n=14)	1813±17 Ma (n=1)
	NAC 2012-21	Augen gneiss	0536998 7332009			1766±10 Ma (n=33)	
	NAC 2011-081	Fine grained muscovite bearing quartzite	0537314 7343111	1311.95 Ma (n=3)	1544.4 Ma (n=12)	1712.17 Ma (n=16)	
West of the Casey Inlier	NAC 2011-072	Granitic gneiss	0524285 7342874		1670±18 Ma (n=25)		
	NAC 2011-073	Muscovite rich leucogranite	0531317 7343637		1660.1± 9.4 Ma (n=33)		
	NAC2011-074	Porphyritic biotite rich granite	0534791 7335421		1652± 13 Ma (n=20)		

Interpretation of Monazite data

Monazites aligned with the upright pervasive NNW-SEE trending fabric, predominantly with the biotite in the matrix; in the Eastern Casey Inlier recording an age of ca1732 Ma. This indicates that deformation occurred during the early Strangways Orogeny. In the Aileron Province, in the east of the Arunta this event is characterised by granulite facies metamorphism. The NNW-SSE trending fabric overprints an earlier high grade metamorphic assemblage. In the Western Domain of the Casey Inlier an identical fabric overprints the ca 1652- 1670 Ma Warumpi Province granites and also the ca 1770 Ma granites in the central domain as well as the granites where there is top to the west shear

sense. This indicates that the Casey Inlier was affected by the ca 1770 Ma Yamba even, which is also supported by the presence of ca 1770 Ma metagabbro's in the Central and Eastern Domain, which show the mixing with the ca 1770 Ma granulite facies migmatites. This also suggests that the Eastern and Central Domain of the Casey Inlier is the same domain, and that the difference in the grade of facies is a result of in the varying intensity of the ca 1730 Ma reworking.

Interpretation of Lu-Hf isotopic data

The metasedimentary rocks NAC 2011-076 and NAC 2011-079 in the Aileron Province range between the source ages of ca 2080- 2810 Ma (appendix c). These samples have U-Pb age evident of inheritance ranging from ca 2230- 2300 Ma. This signature may be isotopically identical but research has suggested that lithopspheric melts producing basaltic rocks can be enriched in composition creating a source region signature that would be identified as the crust. Enrichments of this nature often occur in subduction zones by magmas produced in partial melting (Hergt *et al.* 1989, Hergt *et al.* 1991).

The cover sequence NAC 2011-081 has U-Pb zircon ages that include those of the Warumpi and Aileron Province as well as the Musgrave Province (Figure 12c). The Lu-Hf data is also consistent with derivation of material from the Warumpi and Aileron Province. The increasingly juvenile nature of the younger zircons is also consistent with the higher proportion of young juvenile magmatic rocks in the Musgrave Province (Kirkland *et al.* 2012). The Musgrave Province source range is a younger juvenile source which ranges between the ca1580-2620 Ma (Figure 14a). This is a similar source region to that found by Kirkland *et al*. (2012) (Figure 15) and indicates that the

Musgrave orogeny has exhumed the Musgrave block creating a source region for the muscovite-bearing quartzite sequence found in the Casey Inlier.

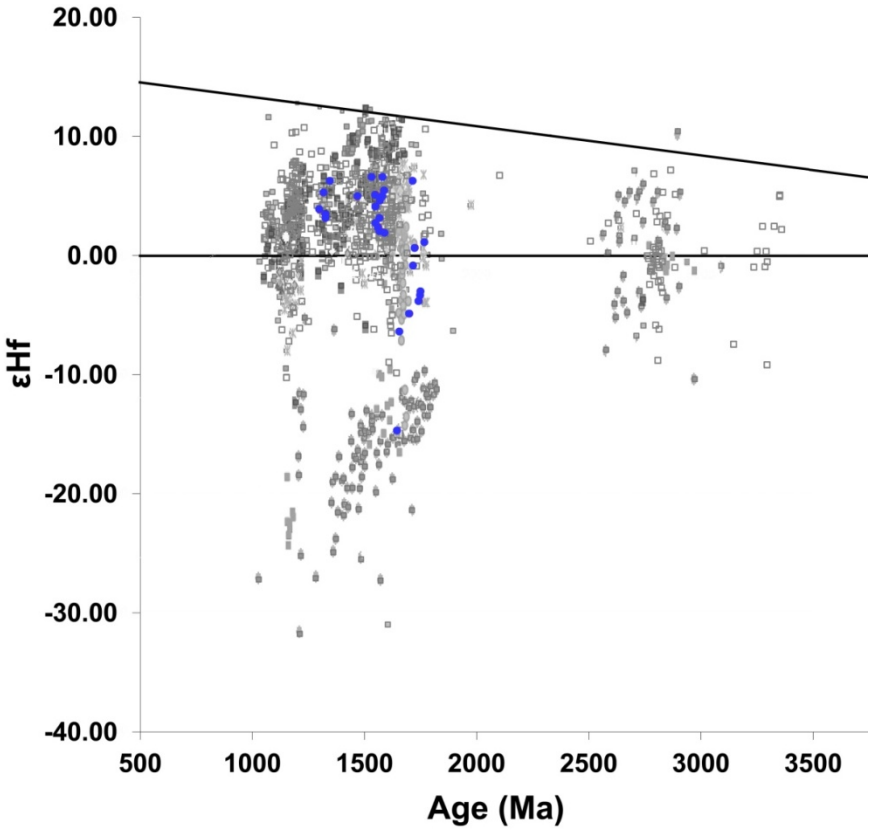

Figure 15: Epsilon Hf against zircon grains 207Pb/206 Pb age. The grey data is Hf compositions from the Musgrave Block (Kirkland et al. 2012). The blue dots are eth cover sequence in the Casey Inlier with a maximum deposition of 1220 Ma, multiply deformed at greenschist (garnet-andalusite) at ca 1150 Ma.

The Aileron Province granites NAC 2012-18 and NAC 2011-077 and the Warumpi Province granites NAC 2011-072, NAC 2011-73 and NAC 200-074 are isotopically indistinguishable and there U-Pb ages are similar (Figure 12d,e and f). The isotopic signature of the mixed juvenile and crustal source of the Warumpi and Aileron Provinces granites, which ranges between ca 2090-2350 Ma (Figure 14a).

Tectonic events that have affect the Casey Inlier

The ca 1756 -1776 Ma granites of the Eastern and Central Domain of the Casey Inlier have been identified as the Aileron Province. There is an increase in age of the granites

from east to west and a decrease in facies grade from high amphibolite to granulite. This indicates an increase in strain and reworking in the Eastern Domain, which has a fabric that has a NNW-SSE fabric with a ca1732 Ma late Strangways event, with east side up kinematic movement. There is an E-W trending fabric which is made up of gentle in the Central Domain, with a retrogressed fabric which is as a result of heating and cooling of the mafic gabbros intruding the domain. There is also combination of east and west side up kinematic movement.

The ca1652-1670 Ma Western Domains identified to be the Warumpi Province, posses the same oriented pervasive NNW-SSE fabric, suggests that it is the same ca 1730 Ma fabric age. There is an invasive west side up kinematic movement indicating that the west is lifting up the further west and increasing in facies grade.

The NNW-SSE fabric in both the Eastern and Western Domain is parallel to the limbs of the macro- isoclinaly folder which is capped by the greenschist, quartzite cover sequence and lies on top of the Aileron Province. Fields pers.comm (2012) Morrissey *et al.* (2011) and Wong (2011) have identified medium to high-grade strain deformation has occurred in the Warumpi Province south of the Aileron Province at a ca 1140Ma. Since the east and west side up shear sense is parallel and the east side up has an age of ca 1730 Ma, this indicates that the west side up shear sense could be the same ca 1140 Ma seen south of the Aileron Province. Further work should be done on constraining the NNW-SSE fabric dates and ages.

Suture model

The magmatic zircon ages in the Eastern and Central Domains of the Casey Inlier, not including the cover sequence, span between ca 1774-1810 Ma. These are common ages in the Aileron Province (Scrimgeour *et al.* 2005). On the western of the Casey Inlier the magmatic ages are younger and span between ca 1650-1670 Ma which correspond magmatic age of the Warumpi Province (Scrimgeour *et al.* 2005). The Aileron and Warumpi Provinces have been proposed to have juxtaposed each other during the ca 1640 Ma Leibig Orogeny (Scrimgeour *et al.* 2005). It has been suggested the Warumpi Province is exotic to the NAC which has been supported by isotopic data indicating that the Warumpi Province had a more juvenile signature (Close *et al.* 2004).

Opposing this zircon Lu-Hf data indicates that the Aileron and Warumpi Provence are isotopically indistinguishable and likely to share the same or similar source region, indicating that the granites in the Wester Domain in the Casey Inlier are not part of an exotic terrain. This supported by the presents of ca 1626- 1663 Ma granites found in the Aileron Province (Fields pers. comm.2012; Lawson-Wyatt pers.comm. 2012; Wong. 2011). The Hf isotopic data indicates that source region of the younger granites is from melts from the Aileron Province, suggesting that the Warumpi Province is a piece of the Aileron Province that has undergone basin development and magmatism between ca 1690-1600 Ma. There is no evidence to suggest that there has been a suture between the Warumpi and Aileron Provinces.

CONCLUSIONS

The ca 1652 -1670 Ma Warumpi Province rocks on the west of the Casey Inlier and the ca 1756-17769 Ma Aileron Province granites in the east of the Casey Inlier are isotopically indistinguishable. Coupled with new evidence for shared magmatic events suggest the two provinces have a shared history. The region has cover sequence with a maximum deposition age of ca 1311 Ma from the Musgrave Province. Pervasive NNW-SSE fabric indicated two deformation events one at ca1730 Ma expressed as east side up shear senses and ca1140 Ma west side up shear sense. There is poor evidence field or source region related data to support that there is a ca 1640 Ma suture between the Warumpi and Aileron Provence.

ACKNOWLEDGEMENTS

I am most sincerely thankful to my supervisors, Martin Hand and Justin Payne for all the help, guidance and support that they have received from them throughout the year. Thank you to the ARC discovery project DP1095456 and ARC linkage project LP100200127 for funding this project. Thank you Martin Kennedy and Rosalind King for all their work supervising the honours year and there guidance. Martin thank you for the most enjoyable field trip, the experience was invaluable and sharing all his knowledge. Thank you to Justin for the countless meeting and intense help with data processing, especially the Lu-Hf work at Whaite Campus, which you gave a lot of time to. Your help is invaluable. A very special thanks to Russell Smith for helping me with all my data collecting and processing and assistance every step of the way. You have been awesome! Thank you David Kelsey for all you help, especially taking the time to teaching me how to use Thermocalc. Thank you to Katie Howard for all the training and help with all the fiddley bits. To Angus Netting and Benjamin Wade for training me on

the New Wave 213 nm, Phillips XL-20 Scanning Electron Microscope and Phillips XL-40 Scanning Electron Microscope in Adelaide Microscopy and constantly help with the machines and taking all my calls at all hours, your help has been invaluable. To Aoife McFadden for training on the New Wave 213 nm , Phillips XL-20 Scanning Electron Microscope and Phillips XL-40 Scanning Electron Microscope the in Adelaide Microscopy, help with all the silly little questions and her constant support. Thank you to Ken Neubauer for coating all my samples especially the ones on short notice and for his quick assistance when I needed an ambulance this year, along with the reception staff. Thank you to Tom Sturman, Farid Shahin, Kathleen Lane and Kathleen Wright for reading through drafts that has been a tremendous help. To Sam Holt and Farid Shahin thank you with all you help making the images. Thank you to all the people in the Continental Evolution Research Group tank for sharing their knowledge and skills.

I would like to thank all the centrals crew in honours for their support and help though out the year. Thank you especially to Farid Shahin, Paige Honor, Maddison Lawson-Wyatt and Sam Holt and all my friends for daily support and encouragement through the year and throughout the ups and downs and support. To all my family, thank you so much for supporting me through the year and believing in me. Thank you to my wonderful housemates Andrea and Alicia for their support, encouragement and patents with me this year.

REFERENCE

BETTS P. G. & GILES D. 2006. THE 1800–1100MA TECTONIC EVOLUTION OF AUSTRALIA. ***PRECAMBRIAN RESEARCH*** **144, 92-125.**

CARSON C. J., CLAOUÉ-LONG J., STERN R. A., CLOSE D. F., SCRIMGEOUR I. R. & GLASS L. M. 2009. ***SUMMARY OF RESULTS. JOINT NTGS-GS GEOCHRONOLOGY PROJECT: ARUNTA AND PINE CREEK REGIONS, JULY 2006-MAY 2007*****. NORTHERN TERRITORY GEOLOGICAL SURVEY, DAWIN.**

CLAOUÉ-LONG J. 2003. ***EVENT CHRONOLOGY IN TEH ARUNTA REGION. ANNUAL GEOSCIENCE EXPLORATION SEMINAR (AGES) 2003. RECORD OF ABSTRACTS. NORTHERN TERRITORY GEOLOGICAL SURVEY RECORD 2003-001*****.**

CLAOUÉ-LONG J., EDGOOSE C. & WORDEN K. 2008. A CORRELATION OF AILERON PROVINCE STRATIGRAPHY IN CENTRAL AUSTRALIA. ***PRECAMBRIAN RESEARCH*** **166, 230-245.**

CLAOUÉ-LONG J. C. & HOATSON D. M. 2005. PROTEROZOIC MAFIC–ULTRAMAFIC INTRUSIONS IN THE ARUNTA REGION, CENTRAL AUSTRALIA: PART 2: EVENT CHRONOLOGY AND REGIONAL CORRELATIONS. ***PRECAMBRIAN RESEARCH*** **142, 134-158.**

CLOSE D., DUFFETT M., SCRIMGEOUR I., WORDEN K. & GOSCOMBE B. 2006. ACCESSING AUSTRALIA'S FINAL EXPLORATION FRONTIER AGES 2006. RECORD OF ABSTRACTS.

CLOSE D., SCRIMGEOUR I., CARSON C. J. & CLAOUÉ-LONG J. 2007. ANNUAL GEOSCIENCE EXPLORATION SEMINAR INCORPORATING THE 2011 MINING S ERVICES EXPO. ***AGES 2007*****.**

CLOSE D., SCRIMGEOUR I. & EDGOOSE C. A. 2004. LATE PALAEOPROTEROZOIC DEVELOPMENT OF THE SW MARGIN OF TEH NORTH AUSTRALIAN CRATON. ***GEOLOGICAL SOCIETY OF AUSTRALIA*** **73, 149.**

COLLINS W. J. & SHAW R. D. 1995. GEOCHRONOLOGICAL CONSTRAINTS ON OROGENIC EVENTS IN THE ARUNTA INLIER: A REVIEW. ***PRECAMBRIAN RESEARCH*** **71, 315-346.**

FIELDS C. E. 2012. ***LIEBIG-AGED (CA. 1640 MA) MAGMATISM AND METAMORPHISM IN CA. 1760 MA CRUST IN THE WARUMPI AND SOUTHERN AILERON PROVINCE, CENTRAL AUSTRALIA: A CASE FOR REVISING THE TECTONIC FRAMEWORK OF PROTEROZOIC AUSTRALIA.B.SC (HONOURS) THESIS, GEOLOGY AND GEOPHYSICS, UNIVERSITY OF ADELAIDE, ADELAIDE (UNPUBL.).***

GILES D., BETTS P. & LISTER G. 2002. FAR-FIELD CONTINENTAL BACKARC SETTING FOR THE 1.80–1.67 GA BASINS OF NORTHEASTERN AUSTRALIA. ***GEOLOGY*** **30, 823-826.**

GILES D., BETTS P. G. & LISTER G. S. 2004. 1.8–1.5-GA LINKS BETWEEN THE NORTH AND SOUTH AUSTRALIAN CRATONS AND THE EARLY–MIDDLE PROTEROZOIC CONFIGURATION OF AUSTRALIA. ***TECTONOPHYSICS*** **380, 27-41.**

GRIFFIN W., POWELL W., PEARSON N. & O'REILLY S. 2008. GLITTER: DATA REDUCTION SOFTWARE FOR LASER ABLATION ICP-MS. ***LASER ABLATION-ICP-MS IN THE EARTH SCIENCES*** **40, 204-207.**

HAND M. & BUICK I. 2001. TECTONIC EVOLUTION OF THE REYNOLDS-ANMATJIRA RANGES: A CASE STUDY IN TERRAIN REWORKING FROM THE ARUNTA INLIER, CENTRAL AUSTRALIA. ***GEOLOGICAL SOCIETY, LONDON, SPECIAL PUBLICATIONS*** **184, 237-260.**

HERGT J. M., CHAPPELL B. W., MCCULLOCH M. T., MCDOUGALL I. & CHIVAS A. R. 1989. GEOCHEMICAL AND ISOTOPIC CONSTRAINTS ON THE ORIGIN OF THE JURASSIC DOLERITES OF TASMANIA. ***JOURNAL OF PETROLOGY*** **30, 841-883.**

HERGT J. M., PEATE D. W. & HAWKESWORTH C. J. 1991. THE PETROGENESIS OF MESOZOIC GONDWANA LOW-TI FLOOD BASALTS. ***EARTH AND PLANETARY SCIENCE LETTERS*** **105, 134-148.**

IDNURM M. 2000. TOWARDS A HIGH RESOLUTION LATE PALAEOPROTEROZOIC - EARLIEST MESOPROTEROZOIC APPARENT POLAR WANDER PATH FOR NORTHERN AUSTRALIA. ***AUSTRALIAN JOURNAL OF EARTH SCIENCES*** **47, 405-429.**

J. W., J. H., M. S., S. E. & R. K. 2004. ZIRCON HF-ISOTOPE ANALYSIS WITH AN EXCIMER LASER, DEPTH PROFILING, ABLATION OF COMPLEX GEOMETRIES, AND CONCOMITANT AGE ESTIMATION. *CHEMICAL GEOLOGY* 209.

JACKSON M., PEARSON N., GRIFFIN W. L. & BELOUSOVA E. A. 2004. THE APPLICATION OF LASER ABLATION-INDUCTIVELY COUPLED PLASMA-MASS SPECTROMETRY TO IN SITU U-PB ZIRCON GEOCHRONOLOGY. *CHEMICAL GEOLOGY* 211, 47-69.

KARLSTROM K. E., ÅHÄLL K. I., HARLAN S. S., WILLIAMS M. L., MCLELLAND J. & GEISSMAN J. W. 2001. LONG-LIVED (1.8–1.0 GA) CONVERGENT OROGEN IN SOUTHERN LAURENTIA, ITS EXTENSIONS TO AUSTRALIA AND BALTICA, AND IMPLICATIONS FOR REFINING RODINIA. *PRECAMBRIAN RESEARCH* 111, 5-30.

KELSEY D. E., HAND M., CLARK C. & WILSON C. 2007. ON THE APPLICATION OF IN SITU MONAZITE CHEMICAL GEOCHRONOLOGY TO CONSTRAINING P–T–T HISTORIES IN HIGH-TEMPERATURE (> 850 C) POLYMETAMORPHIC GRANULITES FROM PRYDZ BAY, EAST ANTARCTICA. *JOURNAL OF THE GEOLOGICAL SOCIETY* 164, 667-683.

KIRKLAND C. L., SMITHIES R. H., WOODHOUSE A. J., HOWARD H. M., WINGATE M. T. D., BELOUSOVA E. A., CLIFF J., MURPHY R. & SPAGGIARI C. V. 2012. CONSTRAINTS AND DECEPTION IN THE ISOTOPIC RECORD; THE CRUSTAL EVOLUTION OF THE WEST MUSGRAVE PROVINCE, CENTRAL AUSTRALIA. *GONDWANA RESEARCH*.

LUDWIG K. R. 2003. USER'S MANUAL FOR ISOPLOT 3.00,. *BERKELEY GEOCHRONOLOGICAL CENTRE, SPECIAL PUBLICATION* 4, 71.

MORRISSEY L., PAYNE J. L., KELSEY D. E. & HAND M. 2011. GRENVILLIAN-AGED REWORKING IN THE NORTH AUSTRALIAN CRATON, CENTRAL AUSTRALIA: CONSTRAINTS FROM GEOCHRONOLOGY AND MODELLED PHASE EQUILIBRIA. *PRECAMBRIAN RESEARCH* 191, 141-165.

PAYNE J. L., FERRIS G., BAROVICH K. M. & HAND M. 2010. PITFALLS OF CLASSIFYING ANCIENT MAGMATIC SUITES WITH TECTONIC DISCRIMINATION DIAGRAMS: AN EXAMPLE FROM THE PALEOPROTEROZOIC TUNKILLIA SUITE, SOUTHERN AUSTRALIA. *PRECAMBRIAN RESEARCH* 177, 227-240.

PAYNE J. L., HAND M., BAROVICH K. M. & WADE B. P. 2008. TEMPORAL CONSTRAINTS ON THE TIMING OF HIGH-GRADE METAMORPHISM IN THE NORTHERN GAWLER CRATON: IMPLICATIONS FOR ASSEMBLY OF THE AUSTRALIAN PROTEROZOIC. *AUSTRALIAN JOURNAL OF EARTH SCIENCES* 55, 623-640.

PIETSCH B. 2001. TOWARDS AN ARUNTA FRAMEWORK. . *ANNUAL GEOSCIENCE EXPLORATION SEMINAR (AGES) 2001. RECIRD OF ABSTRACTS. NORTHERN TERRITORY GEOLOGICAL SURVEY RECORD 2001-001*.

SCHERER E., MUNKER C. & MEZGER K. 2001. CALIBRATION OF THE LUTETIUM–HAFNIUM CLOCK. *SCIENCE* 293, 683–687.

SCRIMGEOUR I. 2003. DEVELOPING A REVISED FRAMEWORK FOR THE ARUNTA REGION. *NTGS ANNUAL GEOSCIENCE EXLORATION SEMINAR (AGES) 2003. RECORD OF ABSTRACTS*.

SCRIMGEOUR I. R., KINNY P. D., CLOSE D. F. & EDGOOSE C. J. 2005. HIGH-T GRANULITES AND POLYMETAMORPHISM IN THE SOUTHERN ARUNTA REGION, CENTRAL AUSTRALIA: EVIDENCE FOR A 1.64 GA ACCRETIONAL EVENT. *PRECAMBRIAN RESEARCH* 142, 1-27.

SEGAL I., HALICZ L. & PLATZNER I. T. 2003. ACCURATE ISOTOPE RATIO MEASUREMENTS OF YTTERBIUM BY MULTIPLE COLLECTION INDUCTIVELY COUPLED PLASMA MASS SPECTROMETRY APPLYING ERBIUM AND HAFNIUM IN AN IMPROVED DOUBLE EXTERNAL NORMALIZATION PROCEDURE. *JOURNAL OF ANALYTICAL ATOMIC SPECTROMETRY* 18, 1217-1223.

SELWAY K., HAND M., HEINSON G. S. & PAYNE J. L. 2009. MAGNETOTELLURIC CONSTRAINTS ON SUBDUCTION POLARITY: REVERSING RECONSTRUCTION MODELS FOR PROTEROZOIC AUSTRALIA. *GEOLOGY* 37, 799-802.

SHAW R., STEWART A. & BLACK L. 1984. THE ARUNTA INLIER: A COMPLEX ENSIALIC MOBILE BELT IN CENTRAL AUSTRALIA. PART 2: TECTONIC HISTORY. *AUSTRALIAN JOURNAL OF EARTH SCIENCES* 31, 457-484.

SLAMA J., KOSLER J., CONDON D. J., CROWLEY J. L., GERDES A., HANCHAR J. M., HHORSTWOOD M S. A., MORRIS G. A., NASDALA L., NORBERG N., SCHALTEGGER U., SCHOENE B., TUBRETT M. N. & WHITEHOUSE M. J. 2008A. PLESOVICE ZIRCON - A NEW NATURAL REFERENCE MATERIAL FOR U-PB AND HF ISOTOPIC MICROANALYSIS. ***CHEMICAL GEOLOGY*** **249, 1-35.**

SLAMA J., KOŠLER J., CONDON D. J., CROWLEY J. L., GERDES A., HANCHAR J. M., HORSTWOOD S. A., A. M. G., NASDALA L., NORBERG N., SCHALTEGGER U., SCHOENE B., TUBRETT M. N. & WHITEHOUSE M. J. 2008B. PLEŠOVICE ZIRCON- A NEW NATURAL REFERENCE MATERIAL FOR U-PB AND HF ISOTOPIC MICROANALYSIS. ***CHEMICAL GEOLOGY*** **249, 1-35.**

VERVOORT J. D., PATCHETT P. J., SÖDERLUND U. & BAKER M. 2004. ISOTOPIC COMPOSITION OF YB AND THE DETERMINATION OF LU CONCENTRATIONS AND LU/HF RATIOS BY ISOTOPE DILUTION USING MC-ICPMS. ***GEOCHEM. GEOPHYS. GEOSYST*** **5, Q11002.**

WADE B. P., BAROVICH K. M., HAND M., SCRIMGEOUR I. R. & CLOSE D. F. 2006. EVIDENCE FOR EARLY MESOPROTEROZOIC ARC MAGMATISM IN THE MUSGRAVE BLOCK, CENTRAL AUSTRALIA: IMPLICATIONS FOR PROTEROZOIC CRUSTAL GROWTH AND TECTONIC RECONSTRUCTIONS OF AUSTRALIA. ***JOURNAL OF GEOLOGY*** **114, 43-63.**

WADE B. P., HAND M., MAIDMENT D. W., CLOSE D. F. & SCRIMGEOUR I. R. 2008. ORIGIN OF METASEDIMENTARY AND IGNEOUS ROCKS FROM THE ENTIA DOME, EASTERN ARUNTA REGION, CENTRAL AUSTRALIA: A U-PB LA-ICPMS, SHRIMP AND SM-ND ISOTOPE STUDY. ***AUSTRALIAN JOURNAL OF EARTH SCIENCES*** **55, 703-719.**

WONG B. L. 2011. GRENVILLIAN-AGED REWORKING OF LATE PALEOPROTEROZOIC CRUST IN THE SOUTHERN AILERON PROVINCE, CENTRAL AUSTRALIA: IMPLICATIONS FOR THE ASSEMBLY OF MESOPROTEROZOIC AUSTRALIA. ***CENTRE FOR TECTONICS, RESOURCES AND EXPLORATION SCHOOL OF EARTH AND ENVIRONMENTAL SCIENCES. THE UNIVERSITY OF ADELAIDE, SOUTH AUSTRALIA*****.**

ZHAO J. & BENNETT V. 1995. SHRIMP U-PB ZIRCON GEOCHRONOLOGY OF GRANITES IN THE ARUNTA INLIER, CENTRAL AUSTRALIA: IMPLICATIONS FOR PROTEROZOIC CRUSTAL EVOLUTION. ***PRECAMBRIAN RESEARCH*** **71, 17-43.**

ZHAO J. & MCCULLOCH M. T. 1995. GEOCHEMICAL AND ND ISOTOPIC SYSTEMATICS OF GRANITES FROM THE ARUNTA INLIER, CENTRAL AUSTRALIA: IMPLICATIONS FOR PROTEROZOIC CRUSTAL EVOLUTION. ***PRECAMBRIAN RESEARCH*** **71, 265-299.**

APPENDICES

Appendix a.

Appendix b.

Appendix c.

*These appendices are contained in a separately attached document called appendices.